HHS Public Access

Author manuscript

Mol Neurobiol. Author manuscript; available in PMC 2017 May 01.

Published in final edited form as:

Mol Neurobiol. 2016 May ; 53(4): 2451–2467. doi:10.1007/s12035-015-9212-4.

Hydrogen Sulfide ameliorates homocysteine-induced Alzheimer's disease-like pathology, blood brain barrier disruption and synaptic disorder

Pradip K. Kamat[#], **Philip Kyles**[#], **Anuradha Kalani**, and **Neetu Tyagi**

Department of Physiology and Biophysics, School of Medicine, University of Louisville, and Louisville, KY 40202, USA.

[#] These authors contributed equally to this work.

Abstract

Elevated plasma total homocysteine (Hcy) level is associated with an increased risk of Alzheimer's disease (AD). During transsulfuration pathways, Hcy is metabolized into hydrogen sulfide (H_2S), which is a synaptic modulator, as well as a neuro-protective agent. However, the role of hydrogen sulfide, as well as NMDAR activation, in hyperhomocysteinemia (HHcy) induced blood-brain barrier (BBB) disruption and synaptic dysfunction, leading to AD pathology is not clear. Therefore, we hypothesized that the inhibition of neuronal NMDA-R by H_2S and MK801; mitigate the Hcy-induced BBB disruption and synapse dysfunction, in part by decreasing neuronal matrix degradation. Hcy intracerebral (IC) treatment significantly impaired cerebral blood flow (CBF), and cerebral circulation and memory function. Hcy treatment also decreases the expression of CBS and CSE in the brain along with increased expression of NMDA-R (NR1) and synaptosomal Ca^{2+} indicating excitotoxicity. Additionally, we found Hcy treatment increased protein and mRNA expression of ICAM-1, MMP-2 and MMP-9 and also increased MMP-2,-9 activity in the brain. The increased expression of ICAM-1, GFAP, and the decreased expression of VE-Cadherin, Claudin-5 indicates BBB disruption and vascular inflammation. Moreover, we also found decreased expression of MAP-2, PSD-95, SAP-97, SNAP-25, synaptophysin, and BDNF showing synapse dysfunction in the hippocampus. Furthermore, NaHS and MK801 treatment ameliorates BBB disruption, CBF, and synapse functions in the mice brain. These results demonstrate a neuro-protective effect of H_2S over Hcy induced cerebrovascular pathology through the NMDA receptor. Our present study clearly signifies the therapeutic ramifications of H_2S for cerebrovascular diseases such as Alzheimer's disease.

Graphical Abstract

Address for Correspondence: Neetu Tyagi, Ph.D. FAPS Department of Physiology and Biophysics, Health Sciences Center, A-1201, University of Louisville Louisville, KY 40202; Phone: 502-852-4145 Fax: 502-852-6239 n0tyag01@louisville.edu.

Conflict of interest: None

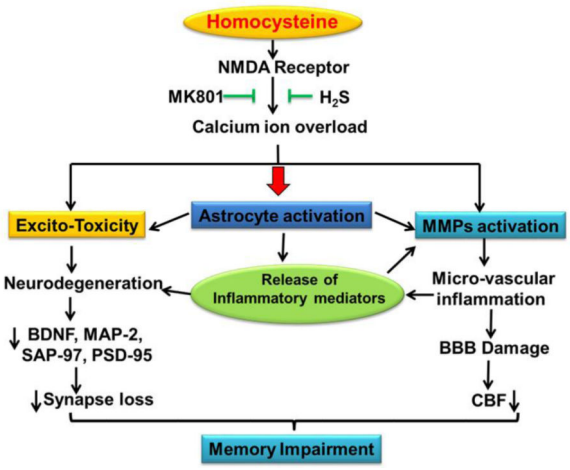

Keywords

Homocysteine; blood brain barrier dysfunction; cerebrovascular pathology; Alzheimer's disease; dementia

1. Introduction

Homocysteine (Hcy) is a toxic thiol-containing molecule, also considered an excitatory amino acid, which markedly enhances the vulnerability of neuronal cells through an excitotoxicity mechanism. An elevated plasma homocysteine level, known as hyperhomocystemia (HHcy), was found to be associated with an increased risk factor for strokes [1], vascular dementia, and Alzheimer's disease (AD) [2-3]. HHcy levels also predict cognitive decline in healthy elderly patients [4-5]. However, not all studies confirm a relationship between Hcy and cognition [6-7]. HHcy's vascular complications and its impact on the hippocampus have not yet been studied. Intriguingly, it has been reported that more than 40% of Alzheimer's disease patients are associated with high plasma Hcy levels which is linked to a more rapid neural atrophy than those with normal levels of Hcy. Therefore, preventing the Hcy induced neurotoxicity may be a novel therapeutic strategy for AD. However, the underlying mechanisms by which Hcy creates an AD-like pathology by means of BBB disruption and altered synapse function are not fully explored.

Hydrogen sulfide (H_2S) is an integral endogenous signaling gasotransmitter molecule. In the brain, H_2S is produced endogenously by the metabolism of the amino acid cysteine (Cys) by the action of cystathionine-β-synthase (CBS) and cystathionine-γ-lyase (CSE). In the mitochondria H_2S is produced by the action of 3-mercaptopyruvate sulfurtransferase enzyme (3-MST). Hydrogen sulfide plays an important role in vasorelaxation, inflammation, cell angiogenesis, hippocampal memory formation, and cellular bioenergetics. Also, it was observed that H_2S levels were decreased and Hcy levels were elevated in AD brains [8]. Likewise it was noted that the physiological concentration of H_2S specifically enhances the NMDA receptor mediated response and facilitates hippocampal long term potentiation (LTP) which is extensively associated with proper learning and memory function.

N-methyl-d-aspartate receptors (NMDARs) are glutamate-gated ion channels that are highly permeable to calcium (Ca^{2+}) and the Ca^{2+} influx through NMDARs is essential for synaptogenesis, synaptic remodeling, and long-lasting changes in synaptic efficacy [9]. The NMDAR is involved in cellular mechanisms for learning and memory function and also plays a role in a wide array of other biological processes crucial for brain development and function [10-11].

Matrix metalloproteinases (MMPs) are a group of zinc-dependent proteolytic enzymes known to be involved in the cleaving of extracellular matrix (ECM) components and pericellular proteins. Among the MMPs: MMP-2, MMP-3 and MMP9 are highly expressed in brain tissues and, like the NMDAR, are associated with various brain functions such as brain development, synaptogenesis, synaptic plasticity, learning and memory, neuron–glia interactions, neuronal injury, and are linked to neuropsychiatric disorders [12-13]. MMP-9 has been extensively characterized and is required for the creation of long-term potentiation (LTP) and plays a vital role in learning and memory through interactions with NMDAR signaling [14-15]. The activation of MMPs leads to the degradation of tight junction (TJ) proteins and consequently causes BBB disruption by degrading the ECM of cerebral blood vessels along with several types of adhesion molecules such as, intra cellular adhesion molecule (ICAM-1) and vascular cell adhesion molecule (VCAM). As expected the BBB damage has a critical role in cerebral pathophysiology and disease progression in the central nervous system [16]. Although MMP-9 role is well known in the regulation of synapse function and plasticity [15, 17], its association with HHcy induced functional remodeling of synapses remains uncertain.

Recently, we have shown that administration of Hcy into the mice brain affects memory function (18) and have shown that H_2S seems to protect against Hcy-induced neurotoxicity, but the underlying pathology was unclear. In our present study we investigated how Hcy induced BBB disruption and altered synapse function. We also scrutinized the relationship between HHcy, the NMDAR, and H_2S as its link to AD-like pathology remains postulated.

2. Methodology

2.1. Antibodies and reagents

Homocysteine, NaHS and MK801 were purchased from Sigma-Aldrich (St. Louis, MO). Antibodies MMP-9, MMP-2, NR1, BDNF, VE-cadherin, MAP-2, Claudin-5, ICAM-1, VCAM-1, PSD-95 and SAP-97 were purchased from ABCAM (Cambridge, MA). HRP-conjugated secondary antibodies were purchased from Santa Cruz Biotechnology (Santa Cruz, CA). Primers of different gene were procured from Invitrogen (Carlsbad, CA). Bradford protein assay reagents, PVDF membrane, and all other chemicals at analytical grade were purchased from Bio-Rad (Hercules, CA).

2.2. Animals

Male wild type (8-10 week old) mice (strain; C57BL/6J) were obtained from Jackson Laboratory (Bar Harbor, ME) and kept in the animal care facility at the University of Louisville where suitable environmental conditions (12:12-h light-dark cycle, 22–24°C)

were maintained. The animals were fed standard food and water ad libitum. All animal procedures were reviewed and approved by the Institutional Animal Care and Use Committee (IACUC) at the University of Louisville School Of Medicine. Moreover, methods and general guidelines for animals use were followed according with Animal Care and Use Program Guidelines of the National Institutes of Health.

2.3. Drug-Preparation and Administration

Hcy was dissolved in freshly prepared artificial cerebrospinal fluid (aCSF; 147 mM NaCl, 2.9 mM KCl, 1.6 mM $MgCl_2$ $6H_2O$, 1.7 mM $CaCl_2$, 2.2 mM dextrose dissolved in distilled water) used as a vehicle for intracerebral administration of Hcy. In the Hcy group a single administration of Hcy (0.5 μM/μl) was given intra-cerebrally (IC) in mice brain. Sodium hydrogen sulfide (NaHS, a H_2S donor) and MK-801 were dissolved in 0.9% normal saline. Hcy (I.C) injected mice were treated with NaHS (30μM/kg/day/i.p) and MK801 (0.05mg/kg/day/i.p) for 7 days through the intraperitoneal route. NaHS and MK801 doses were used as described earlier [18, 19]. Animals of the control group received aCSF intracerebral (IC) injections. Biochemical, behavioral, molecular, and immunohistochemical analyses were done 24 hours after the last NaHS treatment or its vehicle injection in the separate groups.

2.4. Intracerebral (IC) Injection of Hcy

Mice were anesthetized with tribromoethanol anesthetic solution (TB; 2.5 gm, 2,2,2 tribromoethanol (TBE); 5 ml 2-methyl-2-butanol (tertiary amyl alcohol) 200 ml distilled water - neutral pH) (200 μg/gm, i.p). A 27-gauge hypodermic needle attached to a 100 μl Hamilton syringe was inserted (2.5 mM depth) perpendicularly through the skull into the brain. Hcy (0.5μM/μl), dissolved in freshly prepared aCSF, was administered slowly through intracerebral (IC) route. The site of injection was 2 mm from either side of the midline on a line drawn through the anterior base of the ears. We injected Hcy only one side from the midline as previously reported [18]. The syringe was left in the place for a further 2 min for proper diffusion of Hcy.

2.5. Experimental design and drug administration

The mice (n=5 for each study) were grouped as:

aCSF—Mice injected by intracerebral (IC) with artificial cerebrospinal fluid (aCSF) once and treated with vehicles of NaHS and MK-801 for 7 days by intra-peritoneal.

Hcy—Mice were injected IC with Hcy (0.5μM/μl) once and treated with vehicles of NaHS and MK-801 for 7 days by intra-peritoneal.

NaHS *per se*—NaHS (30μM/kg/day) was injected through intra-peritoneal for 7 days in aCSF treated mice.

Hcy+NaHS—NaHS (30μM/kg/day) was injected through intra-peritoneal for 7 days in Hcy (0.5μM/μl) treated mice.

MK801 *per se*—MK801 (0.05mg/kg/day) was injected through intra-peritoneal for 7 days in aCSF treated mice.

Hcy+MK801—MK801 (0.05mg/kg/day) was injected through intra-peritoneal for 7 days in Hcy (0.5μM/μl) treated mice.

2.6. Novel Object Recognition Test

Novel object recognition is a validated and widely used test for assessing recognition memory [20]. Mice were placed individually in a testing chamber with beige walls for a 5 min habituation interval and returned to their home cage. Thirty minutes later mice were placed in the testing chamber for 10 min with two identical objects (acquisition session). Mice were returned to home cages and one day later placed back into the testing chamber in the presence of one of the original objects and one novel object (recognition session) for 5 min. The chambers and objects were cleaned with ethanol between trials. Exploratory behavior was defined as sniffing, touching, and directing attention to the object. Expected normal behavior would be, with a short delay between acquisition and retention trials, that the animal explores the novel object for a longer period of time than the familiar object. For the acquisition session, the recognition index (RI) was calculated as time exploring one of the objects over the time exploring both objects. For the recognition session, the RI was calculated as time exploring the novel object over the time exploring both the familiar and novel object. Discrimination index (DI) is an index of discrimination between object and was calculated by the method described by Kamat et al. [18].

2.7. Passive Avoidance Test

The mice were subjected to the passive avoidance test by placing the animal in a compartment with light at an intensity of 8 [scale from 0 to 10 (brightest)] in a computerized shuttle box with a software program PACS 30 monitoring (Columbus Instruments, OH, USA). The light compartment was isolated from the dark compartment by an automated guillotine door. After an acclimatization period of 30 s, the guillotine door was opened and closed automatically after entry of the mouse into the dark compartment. The subject received a low-intensity foot shock (0.5 mA; 10 s) in the dark compartment. Infrared sensors monitored the transfer of the animal from one compartment to another, which was recorded as transfer latency time (TLT) in seconds. The 1st trial was for acquisition and retention was tested in a 2^{nd} trial and 3^{rd} trial given after 24 and 48 h of the 1st trial. The criteria for learning were taken as an increase in the TLT on retention (2nd or subsequent) trials as compared to acquisition (1st) trial.

2.8. Cerebral Blood Flow

Regional cerebral blood flow (CBF) was measured in the different treatment groups of mice to differentiate the blood flow in brain by using a laser Doppler scan (Moor Instruments, moor FLPI) to verify reperfusion. Briefly skin was gently removed from the cranial surface and cranial window was created by method described by Lominadze et al. [21]. Furthermore the cranium was cleaned with alcohol. CBF of the lateral hemisphere (parietal cortex) was continuously monitored with laser Doppler flowmetry. The head of laser fiber was placed on the area of right hemisphere of the brain. The mice CBF was recorded by software and

calculated by percentage (%) of CBF index (CBFI) = (CBF of Hcy injected mice brain / CBF of aCSF injected mice brain) × 100.

2.9. Microvascular Observation

Microvasculature in the brain was observed through cranial windows and was captured by using a laser Doppler scan (Moor Instruments, moor FLPI). Laser Doppler scans were placed at different areas of the right hemisphere through the cranial window. In brief, cranial window was created with the help of micro driller and parietal bone was removed carefully to avoid any injury. The open area was regularly flushed with aCSF to prevent from drying. After that mouse was placed below the doppler scan to visualize the brain vessel through cranial window.

2.10. Hippocampus Tissue Collection and Protein Extraction

The mice were sacrificed with anesthesia at the end of the memory function test. Brain samples were removed quickly after intra-cardiac perfusion with chilled normal saline and kept on ice-cold PBS immediately. Hippocampal tissue was dissected out by the method of Glowniski and Iversion [22] and used for estimation of biochemical and molecular studies.

2.11. Protein Sample Preparation

Hippocampal tissue samples from each group were weighed and homogenized in 1× RIPA buffer (Tris–HCl 50 mM, pH 7.4; 1% NP-40; 0.25% Na-deoxycholate, 150 mM NaCl; 1 mM EDTA; 1 mM PMSF; 1 μg/ml each of aprotinin, leupeptin, pepstatin; 1 mM Na_3VO_4; 1 mM NaF) containing 1 mM PMSF and 1 μg complete protease inhibitor (Sigma). The homogenate was kept on ice for 30 min and centrifuged (100 g) for 10 minutes at 4°C, and then the supernatant was removed and centrifuged a second time (20,000 g for 15 minutes at 4°C) to remove any remaining debris. Protein levels for all samples were quantified by the Bradford method (Bio-Rad,CA) and stored at −80°C for further use.

2.12. RNA Sample Preparation and RT-PCR Analysis

RNA samples from the hippocampal tissues were prepared by the Trizol method. The quantity and quality of RNA was measured using a Nano Drop 1000 spectrophotometer and the purity of the RNA was determined by A260/A280 ratio. Approximately 2 μg of total RNA was reverse transcribed using reverse transcriptase (RT) in a 20 μl mixture containing oligo(dT) primer, RNase Inhibitor, dNTP mix, and 5x reaction buffer (Omniscript QIAGEN Inc. Valencia, CA, U.S.A.). RT-PCR reaction was performed by using ImProm-II™ Reverse Transcription PCR system kit (Promega Corporation, Madison, WI). Complimentary DNA (cDNA) was prepared by using 2 μg of the isolated RNA. A reverse transcription program on the DNA Engine S1000 Thermal Cycler (Bio-Rad Laboratories, Hercules, CA) was used to make the cDNA. The transcript level of gene expression was determined in the cDNA sample by using Reverse transcriptase PCR. The PCR mixture (25 μl) contained PCR master mix, 2 μl cDNA and 40 pMol primer and amplified through stratagene Mx3000p (Agilent Technologies, Santa Clara, CA, USA). The gene expression in all the groups was normalized with GAPDH expression.

2.13. Micro Vascular Permeability in Brain

Blood flow in the brain microvasculature was measured in anesthetized mice fitted in a stereotaxic apparatus to prevent mechanical damage during drilling. A cranial window was made in the skull using a high speed micro drill (Fine Surgical Tool). The exposed area was regularly flushed with artificial cerebrospinal fluids. Syringe pumps were fitted with two injections, one containing heparin saline to prevent from clotting and the other with an FITC solution. Fluorescein isothiocyanate (300mg/ml) bound to BSA (FITC-BSA) was infused (0.2 mL/100 g of body wt.) by a syringe pump (Harvard Apparatus) and allowed to circulate for about 5 minutes [21]. The pial circulation was surveyed to ensure that spontaneous leakage in the observed area would not falsely indicate vascular integrity. Venules were identified by observing the topology of the pial circulation and blood flow direction (vascular diameters increasing in the direction of blood flow). The exposed area was actively observed using in vivo imaging fluorescent microscopy (Olympus, Japan).

2.14. Immunohistochemistry

The frozen brain tissues were blocked with blocking solution (5% BSA in TBS-T) and incubated with a primary antibody at 1:100 dilutions overnight at 4 °C. The unbound antibody was washed with TBS and the sections then incubated with goat anti-mouse alexa flour 488 and goat anti-rabbit taxas red for 60 min at RT. The slides were further stained with DAPI (1:10,000) for 10 min, was washed, and mounted with anti-fade mounting media. The images were acquired using a laser scanning confocal microscope (60 × objectives, FluoView 1000, Olympus, PA, USA). Total fluorescence intensity in five random fields (for each experiment) was measured with image analysis software (Image-Pro Plus, Media Cybernetics, and Rockville, MD, USA).

2.15. Western Blotting

Western blot analysis was used for protein expression in the different treatment groups. Briefly, protein was extracted using 1x RIPA buffer. Equal amounts of protein from the brains were separated by SDS-PAGE. Further, the proteins from the gel were transferred onto PVDF membranes to check their expression (BioRad, Hercules, CA) by wet transfer method. Non-specific sites of protein on membrane were blocked with 5% non-fat dry milk in TBS-T (50 mM Tris–HCl, 150 mM NaCl, 0.1% Tween- 20, pH 7.4) for 1 h at room temperature at slow rocking. The membranes were washed with washing buffer (pH 7.6, TBS, 0.1% Tween 20) three times at 10 min. each. The blots were then incubated overnight at 4°C with the appropriate primary antibody prepared in TBS-T solution. The blots were washed with TBS-T (3 times, 10 min each) and incubated with appropriate HRP- conjugated secondary antibody for 2 hrs at room temperature. After washing with TBST-T, ECL Plus substrate (Thermo scientific, inc.) was applied to the blot for protein expression and images were captured in the gel documentation system. Relative optical density of protein bands were analyzed by using software image lab 3.0. The same membranes were stripped and re-probed with GAPDH as a loading control.

2.16. Gelatin Zymography

Brain samples were minced in an ice-cold extraction buffer (1:3 w/v) containing 10 mMol/l cacodylic acid, 20 mM ZnCl, 1.5 mM NaN_3, and 0.01% Triton X-100 (pH 5.0) and incubated overnight at 4°C with gentle agitation. The homogenate was centrifuged for 15 min at 1500 x g and the supernatant was collected. 50 μg of the protein was electrophoretically resolved for each sample in 10% SDS-PAGE containing 0.1% gelatin as the MMP substrate. Gels were washed in renaturing buffer with one change in between to remove the SDS, rinsed in water, and incubated for at least 48 hrs in developing buffer at 37°C in a water bath with gentle shaking. Gels were stained with 0.5% Coomassie brilliant blue for 1 h at room temperature. MMP activity in the gel was detected as white bands against a dark blue background.

2.17. Statistical Analysis

The results were expressed as mean ± S.E.M. Memory functions were analyzed by ANOVA followed by a student T test. Biochemical and molecular data were analyzed by a student T test. A *p value* $p<0.05$ was considered to be significant. The data were analyzed by using software graph pad prism version X6.

3. Results

3.1. Memory Function by Passive Avoidance Test (PAT)

3.1.1. Effect of NaHS and MK801 on Hcy Induced Memory Impairment—A test was performed to assess the memory function in the mice of different groups. We did not found significant difference in transfer latency time in retention trial of day 1 and day 2 as compared to the acquisition trial in Hcy injected mice. However treatment with H_2S donor (NaHS) and NMDA receptor antagonist (MK801) significantly increased the transfer latency time in Hcy injected mice. Further, we did not observe any alteration in H_2S and MK801 *per se* treated group on memory function as compared to aCSF treated group (Fig. 1A).

3.1.2. Novel Object Recognition Test—The novel object recognition test was performed for determining memory function in mice. Hcy (IC) treated mice exhibit significantly impaired novel object recognition performance in the simple task relative to wild type mice exploring the novel object. There was no change in recognition index (RI) in the acquisition trial among the group, but significant changes were observed in the retention trial. Consistent with the lack of net preference between novel and familiar objects, the discrimination index (DI) in Hcy treated mice was reduced with respect in the wild types. NaHS and MK-801 treatment led to improved preference between novel and familiar object in Hcy treated mice (Fig. 1B).

3.2. Effect of NaHS and MK801 on Hcy Induced Physiological Properties of Micro-Vessel and

3.2.1. Microvascular Density—Angiogenesis is a complex process that involves an appropriate environment of the brain. This environment requires the proper presence of extracellular matrix proteins, proteases, and the occurrence of other cellular events in sequential order. In the Hcy injection group, microvascular density was significantly less

after seven days post treatment. Treatment with NaHS and MK801 significantly restored microvascular density in Hcy-injected mice brain and indicates the angiogenic properties of NaHS and MK801. Further, we did not observe any change in microvascular density either with MK801, or hydrogen sulfide *per se* treatments (Fig. 2A).

3.2.2. Cerebral Blood Flow (CBF)—CBF, which is necessary for maintenance of the brain function, was assessed in different treatment groups. There was significant decreased blood flow in Hcy treated mice as compared to the aCSF treated group. Interestingly, the given treatment of hydrogen sulfide and MK801 significantly alleviated blood flow in Hcy-injected mice brain. However, no changes were found in *per se* treatment with hydrogen sulfide donor and MK801 treatments (Fig. 2B)

3.2.3. Microvascular Permeability—Typically, a balance occurs between the amounts of plasma going into the tissues from the microvascular capillaries and the amount re-entering the circulatory system from the tissues. When the neuronal tissue is damaged as a result of injury, the lining of the small blood vessels becomes leaky, thereby increasing vessel permeability and disturbing normal brain function. Hcy (IC) injection in mice brain caused an increase of permeability in the micro vessels as evidenced by BSA (FITC) leakage when compared to aCSF injected mice. Interestingly, NaHS and MK801 treatment significantly protected the apparent leakage of BSA (FITC) indicating a vascular-protective effect. There was no significant change in permeability of mice brain with respect to the NaHS and MK801 *per se* treatments (Fig. 3A-B).

3.3. Effect of NaHS and MK801 on H_2S Metabolizing Enzyme (CBS and CSE) Expression

CBS and CSE act on substrates Hcy and L-cysteine to produce H_2S. In cases of excess Hcy, redox stress imbalance occurs and affects CBS and CSE gene expression. We observed a decreased expression of CBS and CSE in the hippocampus of the Hcy injected mouse brains. Conversely, the expression of CBS and CSE was restored by NaHS and MK801 treatment. However, no changes were found in the expression pattern of CBS and CSE in NaHS and MK801 *per se* groups (Fig. 4A-B).

3.4. Effect of NaHS and MK801 on Hcy Induced MMPs Neurophysiological MMP-2 and 9 Expression and Activity

Matrix metalloproteinase (MMPs)-2 and -9, also called gelatinases A and B, play a vital role in the degradation of the BBB and consequently can cause neuronal impairment in the brain if overstimulated. Hcy (IC) injection led to increased MMP-9 and MMP-2 proteins and mRNA expression respectively in the hippocampus. Hydrogen sulfide and MK801 significantly mediated the elevation of MMP-9 and MMP-2 expression whereas the per se treatment with hydrogen sulphide or MK801 did not show any effect on MMP proteins or mRNA expression. The zymography assay showed increased activity of MMP-9 and MMP-2 in Hcy treated mice brain hippocampus as compared to aCSF group. The treatment with NaHS and MK801 significantly mitigated the expression and activity of MMP-9 and MMP-2 induced by Hcy. No changes were found in the *per se* treatments of NaHS and MK801 (Fig. 5A-F).

3.5. Effect of NaHS and MK801 on Hcy Induced Altered Neurovascular Remodeling ICAM-1 and Claudin-5 Protein and mRNA Expression

Altered expression of Caludin-5 and ICAM-1 misbalances the BBB equilibrium and can promote the formation of leaky blood vessels by means of enhanced leukocyte extravasation. Intra-cerebral injection of Hcy caused significant increases in ICAM-1 protein and mRNA expression and decreased protein and mRNA expression of Claudin-5 suggesting vascular inflammation and disruption. Further, treatment with NaHS and MK801 significantly ameliorated these abnormalities. No changes were observed in ICAM-1 and Claudin-5 protein and mRNA expression with *per se* treatment of NaHS and MK801 (Fig. 6A-D).

3.6. Immunohistochemistry of ICAM-1 and Claudin-5

Immunohistochemistry assay showed differential expression of ICAM-1 and Claudin-5 in Hcy (IC) injected mouse brain. Briefly, we found increased expression of ICAM-1 and decreased expression of Claudin-5 which was significantly improved by NaHS and MK801 treatment. No difference was observed with NaHS and MK801 *per se* treatments (Fig. 6E-F).

3.7. Western blotting, mRNA Expression and Immunohistochemistry of GFAP and VE-Cadherin

Endothelial permeability is synchronized in part by the dynamic opening and closure of cell to cell adherens junctions (AJs). Increased vascular permeability affects the function and organization of VE-cadherin and other proteins such as GFAP. Western blot and PCR analysis showed increased expression of GFAP and decreased expression of VE Cadherin in Hcy injected mice brain. Additionally, NaHS and MK801 treatment significantly improved the expression of GFAP and VE Cadherin. No alteration was observed with NaHS and MK801 *per se* treatment. Immunohistochemistry assay also showed altered expression of GFAP and VE cadherin in Hcy injected mice brain as compared to aCSF injected mice brain. Treatment with NaHS and MK801 for seven days significantly *restored* their appropriate expression. Moreover, no significant changes were found in GFAP and VE cadherin expression of NaHS and MK801 *per se* treatment groups (Fig. 7A-F).

3.8. Effect of NaHS and MK801 on Hcy Induced Altered Synapse NR1 and BDNF Protein and mRNA Expression

Intracerebral injection of Hcy caused increased expression of NR1 protein and NR1 mRNA and decreased the expression of BDNF protein and BDNF mRNA. In addition to that, *per se* treatments with both the reagents did not showed and difference. Further, treatment with NaHS and MK801 treatment significantly restored the protein and mRNA expression of NR1 and BDNF (Fig. 8A-F).

3.9. Synaptosomal Ca^{2+} level

Calcium ions maintain synapse plasticity and regulate synaptic function in neurons. In the present study, Hcy caused an increase in Ca^{2+} levels in the synapse preparation which was normalized in our NaHS and MK-801 treatment groups. No considerable changes were observed in MK-801 and NaHS treatment (Fig. 9).

3.10. MAP-2 mRNA and Protein Expression

MAP-2 is found in neuronal dendrites and is involved in microtubule assembly within the brain. Western blot and PCR assay depicts altered protein and mRNA expression of MAP-2 in the hippocampus of Hcy injected mouse brain in comparison to aCSF injected mouse brain hippocampus. Likewise, NaHS and MK801 significantly restored MAP-2's expression. The treatments of both NaHS and MK801 did not show any difference in the *per se* groups (Fig. 10AD).

3.11. PSD-95 and SAP-97 Protein Expression

PSD-95 and SAP-97 are scaffolding proteins that have been implicated in the regulation of synapse function. Both the synapse markers PSD-95 and SAP-97 were down regulated in the hippocampus of Hcy injected mouse brain. Conversely, the expression of PSD-95 and SAP-97 was restored by NaHS and MK801 treatments. No difference was found in the expression pattern of PSD-95 and SAP-97 in NaHS and MK801 *per se* treatment groups (Fig. 11A-D).

3.12. Immunohistochemistry of MMP-9 and SAP-97

Immunohistochemistry analysis showed increased expression of MMP-9 and decreased expression of SAP-97 in Hcy (IC) injected mouse brain. Further, NaHS and MK801 treatment significantly improved the expression of MMP-9 and SAP-97. No difference was observed with NaHS and MK801 *per se* treatments (Fig. 12A-B).

3.13. SNAP-25, Synaptophysin and PSD-95 mRNA Expression

In RT PCR study; we found a significant decrease in SNAP-25, Synaptophysin and PSD-95 expression in Hcy injected mouse brain hippocampus. Interestingly, treatment with NaHS and MK801 significantly restored the synapse as evidenced by the increased expression of SNAP-25, Synaptophysin, and PSD-95 in the hippocampus indicating the potential protective effect of H_2S over the altered synapse function (Fig. 13A-B).

4. Discussion

Increased plasma homocysteine (Hcy) levels are a known risk factor for cerebrovascular disease and have been reported in association with cognitive impairment [23]. Reports suggested that high homocysteine levels also affect blood flow through vessels. Moreover, decreased cerebral blood flow (CBF) is associated with cognitive impairment and Alzheimer's disease (AD) as well as other types of dementia [24-25]. Previous reports also suggested the relationship between CBF and brain function by showing that an increase in CBF is beneficial for cognitive function [26-27]. Concurrent with the above study; we observed a significant decrease in CBF and impaired memory function in Hcy-injected mice brain. Treatment with NaHS and MK801 significantly improved CBF and memory functions in our study. Protection offered by NaHS and MK801 may be due to increased CBF and improved synaptic plasticity.

Moreover, our results also pointed out relationships and interactions between the NMDA receptor and hydrogen sulfide (H_2S) as we observed protection from both therapeutic agents

assumingly mitigated by their effects on the NMDAR. To further confirm the relationship of H_2S and NMDA-R1, we estimated the NR1 expression in different experimental groups. Interestingly, we found that NaHS and MK801significantly ameliorate increased NR1 expression in Hcy-injected mice. These results strongly suggest the interaction between hydrogen sulfide and NMDA receptor and provide a plausible protective mechanism of H_2S. On the other hand we also found decreased expression of H_2S metabolizing enzyme CBS and CSE in mice hippocampus region indicate the low production of H_2S. Further Treatment with MK801 and NaHS significantly ameliorates the CBS and CSE expression.

Previous reports have shown that the alteration of microvascular permeability and disruption of the BBB are detected in the brains of AD subjects and is one of the major events of AD [28]. Concurrent with this reports we also found that intracerebral injection of Hcy caused increased BSA-FITC leakage which indicates BBB disruption and increased microvascular permeability. Further, NaHS and MK801 significantly inhibited BSA-FITC leakage which shows the potential of H_2S in maintaining microvascular permeability (preventing BBB disruption). Kook et.al [29] reported that perturbed intracellular Ca^{2+} homeostasis and BBB damage has implication in the pathogenesis of AD. Disturbed Ca^{2+} homeostasis can also affect synaptic plasticity. In agreement with these reports we also observed increased synaptosomal Ca^{2+} levels indicating excitotoxicity and altered synapse function in Hcy treated groups, interestingly, NaHS and MK801 treatment significantly alleviated the Ca^{2+} influx and thus maintains synapse function. This result further indicates the role of the NMDA receptor in BBB disruption and protective role of H_2S in e BBB disruption during HHcy mouse brain.

Earlier reports suggest that MMPs may be involved in a variety of cellular functions in the brain depending on the cell type involved and up regulation of MMP-9 may contribute to the pathogenesis of neurodegenerative disorders [30, 31]. Moreover, synapse remodeling induced by MMPs can be blocked by the NMDAR antagonist MK-801, indicating role of NMDAR in synapse remodeling. Nagy et al. [17] suggested the role of MMP-9 in learning and memory. We also found increased levels of MMP-2 and MMP-9 expression as well as increased MMP-9 activity in the hippocampus of Hcy injected mouse brain. Further, treatment with NaHS and MK801 reduces MMP-2,-9 expression as well as their activity in the hippocampus indicating that MMPs are associated with NMDAR activity within the memory center.

Increased MMPs expression leads to disruption of tight junction (TJ) proteins by their natural degradation activity. The BBB permeability depends on the TJ proteins that are present between the endothelial cells of the brain capillaries which provide a secure environment for the brain and astrocytes [32]. Claudin-5 is the major TJ protein involved in the maintenance of BBB integrity. Our result showed decreased expression of claudin-5 in an Hcy injected mouse brain, which indicates that BBB integrity was disrupted; however BBB integrity was restored by NaHS and MK801 treatments. Loss of BBB integrity is associated with increased vascular inflammation in cerebrovascular disease. Intracellular adhesion molecule (ICAM-1) expression is restricted to vascular endothelial cells [33] and can be overexpressed in a variety of cells, including neurons, under inflammatory conditions. Indirect evidence from other studies also suggests that high level of ICAM-1

expression in brain tissues is linked with AD and stroke [34]. In accordance with the above reports Hcy also induced ICAM-1 expression in the mouse hippocampus. Interestingly, overexpression of ICAM-1 was mitigated by NaHS and MK801 treatment. We also checked the expression of astrocyte proteins which has been extensively associated with inflammation and nutritional equilibrium in neurons. Astrocyte activation is usually associated with synapse dysfunction in pathological conditions of the brain [35]. In our experiments, we found increased expression of GFAP in Hcy injected mouse brain which strongly indicates astrocyte activation. To confirm this increase, we performed immunohistochemistry of astrocytes by GFAP and VE-Cadherin (an adherence junction protein associated with blood vessels). We found an increased level of GFAP and decreased level of VE-Cadherin protein indicates an association of astrocyte activation with vascular dysfunction. Further, to investigate the correlation of astrocytes with synaptic function and memory, we estimated the pre-synapse and post-synapse markers (synaptophysin, SNAP-25, SAP-97, PSD-95 and MAP-2) and brain derived nerve factor (BDNF) in the hippocampal tissues. Neurite marker MAP-2 and PSD-95 associated with synaptic transmission, synaptic plasticity and also maintains synaptogenesis [35, 36]; while synapse-associated protein 97 (SAP-97) exhibits protein interactions, and localization of synaptic, presynaptic, and dendritic proteins. These synapse proteins are extensively involved in maintaining neuronal function and synapse function. Similar to vascular inflammation, synaptic dysfunction is also believed to play an important role in the pathogenesis of AD [37] and the altered intensity of the synaptic proteins may underlie memory impairment [38]. Other reports reinforce that changes in synapse function are central to AD progression and the loss of synaptic plasticity occurring in the learning and memory process [39-40]. To check the synaptic changes in Hcy induced altered learning and memory processes; we checked the expression of synaptic proteins and mRNA expression in the different groups of treatment. In agreement with the previously mentioned reports, we also found a significant decrease in synaptophysin, SNAP-25, SAP-97, PSD-95, MAP-2, and BDNF levels indicating synaptic changes within the neurons. This data clearly demonstrates that Hcy leads to synaptic remodeling in the hippocampus. Treatment with NaHS and MK801 significantly ameliorates the level of synaptophysin, SNAP-25, SAP-97, PSD-95, MAP-2 and BDNF in the mouse hippocampus. Thus, our present study clearly indicates the therapeutic potential of H_2S on synaptic remodeling. Additionally, this data may be critical to better understand the role of MMPs in neurovascular injury in hyperhomocysteinemia. However, more detailed studies using this model may be warranted to more closely simulate the clinical scenario in cerebrovascular disease such as Alzheimer's and stroke.

Acknowledgment

Financial support from National Institutes of Health grants HL107640-NT is greatly acknowledged.

References

1. Brustolin S, Giugliani R, Felix TM. Genetics of homocysteine metabolism and associated disorders. Braz J Med Biol Res. 2010; 43:1–7. [PubMed: 19967264]
2. Nilsson K, Gustafson L, Hultberg B. Plasma homocysteine and cognition in elderly patients with dementia or other psychogeriatric diseases. Dement Geriatr Cogn Disord. 2010; 30:198–204. [PubMed: 20798540]

3. Seshadri S, Beiser A, Selhub J, Jacques PF, Rosenberg IH, D'Agostino RB, Wilson PW, Wolf PA. Plasma homocysteine as a risk factor for dementia and Alzheimer's disease. N Engl J Med. 2002; 346:476–83. [PubMed: 11844848]

4. McCaddon A, Hudson P, Davies G, Hughes A, Williams JH, Wilkinson C. Homocysteine and cognitive decline in healthy elderly. Dement Geriatr Cogn Disord. 2001; 12:309–13. [PubMed: 11455131]

5. McCaddon A, Regland B. Homocysteine and cognition--no longer a hypothesis? Med Hypotheses. 2006; 66:682–3. [PubMed: 16298495]

6. Luchsinger JA, Tang MX, Shea S, Miller J, Green R, Mayeux R. Plasma homocysteine levels and risk of Alzheimer disease. Neurology. 2004; 62:1972–6. [PubMed: 15184599]

7. Ravaglia G, Forti P, Maioli F, Scali RC, Saccheitti L, Talerico T, Mantovani V, Bianchin M. Homocysteine and cognitive performance in healthy elderly subjects. Arch Gerontol Geriatr Suppl. 2004; 9:349–57. [PubMed: 15207433]

8. Zhuo JM, Wang H, Pratico D. Is hyperhomocysteinemia an Alzheimer's disease (AD) risk factor, an AD marker, or neither? Trends Pharmacol Sci. 2011; 32:562–71. [PubMed: 21684021]

9. Collingridge GL, Isaac JT, Wang YT. Receptor trafficking and synaptic plasticity. Nat Rev Neurosci. 2004; 5:952–62. [PubMed: 15550950]

10. Perez-Otano I, Ehlers MD. Learning from NMDA receptor trafficking: clues to the development and maturation of glutamatergic synapses. Neurosignals. 2004; 13:175–89. [PubMed: 15148446]

11. Rai S, Kamat PK, Nath C, Shukla R. A study on neuroinflammation and NMDA receptor function in STZ (ICV) induced memory impaired rats. J Neuroimmunol. 2013; 254:1–9. [PubMed: 23021418]

12. Lee SH, Sharma M, Sudhof TC, Shen J. Synaptic function of nicastrin in hippocampal neurons. Proc Natl Acad Sci U S A. 2014; 111:8973–8. [PubMed: 24889619]

13. Ethell IM, Ethell DW. Matrix metalloproteinases in brain development and remodeling: synaptic functions and targets. J Neurosci Res. 2007; 85:2813–23. [PubMed: 17387691]

14. Bozdagi O, Nagy V, Kwei KT, Huntley GW. In vivo roles for matrix metalloproteinase-9 in mature hippocampal synaptic physiology and plasticity. J Neurophysiol. 2007; 98:334–44. [PubMed: 17493927]

15. Michaluk P, Mikasova L, Groc L, Frischknecht R, Choquet D, Kaczmarek L. Matrix metalloproteinase-9 controls NMDA receptor surface diffusion through integrin beta1 signaling. J Neurosci. 2009; 29:6007–12. [PubMed: 19420267]

16. Kalani A, Kamat PK, Tyagi SC, Tyagi N. Synergy of homocysteine, microRNA, and epigenetics: a novel therapeutic approach for stroke. Mol Neurobiol. 2013; 48:157–68. [PubMed: 23430482]

17. Nagy V, Bozdagi O, Matynia A, Balcerzyk M, Okulski P, Dzwonek J, Costa RM, Silva AJ, Kaczmarek L, Huntley GW. Matrix metalloproteinase-9 is required for hippocampal late-phase long-term potentiation and memory. J Neurosci. 2006; 26:1923–34. [PubMed: 16481424]

18. Kamat PK, Kalani A, Givvimani S, Sathnur PB, Tyagi SC, Tyagi N. Hydrogen sulfide attenuates neurodegeneration and neurovascular dysfunction induced by intracerebral-administered homocysteine in mice. Neuroscience. 2013; 252:302–19. [PubMed: 23912038]

19. Kamat PK, Rai S, Swarnkar S, Shukla R, Ali S, Najmi AK, Nath C. Okadaic acid-induced Tau phosphorylation in rat brain: role of NMDA receptor. Neuroscience. 2013; 238:97–113. [PubMed: 23415789]

20. Lyon L, Saksida LM, Bussey TJ. Spontaneous object recognition and its relevance to schizophrenia: a review of findings from pharmacological, genetic, lesion and developmental rodent models. Psychopharmacology (Berl). 2012; 220:647–72. [PubMed: 22068459]

21. Lominadze D, Tyagi N, Sen U, Ovechkin A, Tyagi SC. Homocysteine alters cerebral microvascular integrity and causes remodeling by antagonizing GABA-A receptor. Mol Cell Biochem. 2012; 371:89–96. [PubMed: 22886392]

22. Glowinski J, Iversen LL. Regional studies of catecholamines in the rat brain. I. The disposition of [3H]norepinephrine, [3H]dopamine and [3H]dopa in various regions of the brain. J Neurochem. 1966; 13:655–669. [PubMed: 5950056]

23. Ravaglia G, Forti P, Maioli F, Zanardi V, Dalmonte E, Grossi G, Cucinotta D, Macini P, Caldarera M. Blood homocysteine and vitamin B levels are not associated with cognitive skills in healthy normally ageing subjects. J Nutr Health Aging. 2000; 4:218–22. [PubMed: 11115804]
24. O'Brien JT, Eagger S, Syed GM, Sahakian BJ, Levy R. A study of regional cerebral blood flow and cognitive performance in Alzheimer's disease. J Neurol Neurosurg Psychiatry. 1992; 55:1182–7. [PubMed: 1479398]
25. Prohovnik I, Mayeux R, Sackeim HA, Smith G, Stern Y, Alderson PO. Cerebral perfusion as a diagnostic marker of early Alzheimer's disease. Neurology. 1988; 38:931–7. [PubMed: 3368076]
26. Nash DT, Fillit H. Cardiovascular disease risk factors and cognitive impairment. Am J Cardiol. 2006; 97:1262–5. [PubMed: 16616038]
27. Tota S, Kamat PK, Awasthi H, Singh N, Raghubir R, Nath C, Hanif K. Candesartan improves memory decline in mice: involvement of AT1 receptors in memory deficit induced by intracerebral streptozotocin. Behav Brain Res. 2009; 199:235–40. [PubMed: 19103228]
28. Claudio L. Ultrastructural features of the blood-brain barrier in biopsy tissue from Alzheimer's disease patients. Acta Neuropathol. 1996; 91:6–14. [PubMed: 8773140]
29. Kook SY, Seok Hong H, Moon M, Mook-Jung I. Disruption of blood-brain barrier in Alzheimer disease pathogenesis. Tissue Barriers. 2013; 1:e23993. [PubMed: 24665385]
30. Rosenberg GA. Matrix metalloproteinases in neuroinflammation. Glia. 2002; 39:279–91. [PubMed: 12203394]
31. Yong VW, Power C, Forsyth P, Edwards DR. Metalloproteinases in biology and pathology of the nervous system. Nat Rev Neurosci. 2001; 2:502–11. [PubMed: 11433375]
32. Foster CA, Mechtcheriakova D, Storch MK, Balatoni B, Howard LM, Bornancin F, Wlachos A, Sobanov J, Kinnunen A, Baumruker T. FTY720 rescue therapy in the dark agouti rat model of experimental autoimmune encephalomyelitis: expression of central nervous system genes and reversal of blood-brain-barrier damage. Brain Pathol. 2009; 19:254–66. [PubMed: 18540945]
33. Frohman EM, Frohman TC, Gupta S, de Fougerolles A, van den Noort S. Expression of intercellular adhesion molecule 1 (ICAM-1) in Alzheimer's disease. J Neurol Sci. 1991; 106:105–11. [PubMed: 1685745]
34. Wilker EH, Alexeeff SE, Poon A, Litonjua AA, Sparrow D, Vokonas PS, Mittleman MA, Schwartz J. Candidate genes for respiratory disease associated with markers of inflammation and endothelial dysfunction in elderly men. Atherosclerosis. 2009; 206:480–5. [PubMed: 19409562]
35. Rai S, Kamat PK, Nath C, Shukla R. Glial activation and post-synaptic neurotoxicity: the key events in Streptozotocin (ICV) induced memory impairment in rats. Pharmacol Biochem Behav. 2014; 117:104–17. [PubMed: 24333387]
36. Kamat PK, Rai S, Swarnkar S, Shukla R, Nath C. Mechanism of synapse redox stress in Okadaic acid (ICV) induced memory impairment: Role of NMDA receptor. Neurochem Int. 2014; 76:32–41. [PubMed: 24984170]
37. Lee H, Lee EJ, Song YS, Kim E. Long-term depression-inducing stimuli promote cleavage of the synaptic adhesion molecule NGL-3 through NMDA receptors, matrix metalloproteinases and presenilin/gamma-secretase. Philos Trans R Soc Lond B Biol Sci. 2014; 369:20130158. [PubMed: 24298159]
38. Li W, Yu J, Liu Y, Huang X, Abumaria N, Zhu Y, Huang X, Xiong W, Ren C, Liu XG, Chui D, Liu G. Elevation of brain magnesium prevents synaptic loss and reverses cognitive deficits in Alzheimer inverted question marks disease mouse model. Mol Brain. 2014; 7:65. [PubMed: 25213836]
39. Spires-Jones TL, Hyman BT. The intersection of amyloid beta and tau at synapses in Alzheimer's disease. Neuron. 2014; 82:756–71. [PubMed: 24853936]
40. van der Zee EA. Synapses, spines and kinases in mammalian learning and memory, and the impact of aging. Neurosci Biobehav Rev. 2014; 50C:77–85. [PubMed: 24998408]

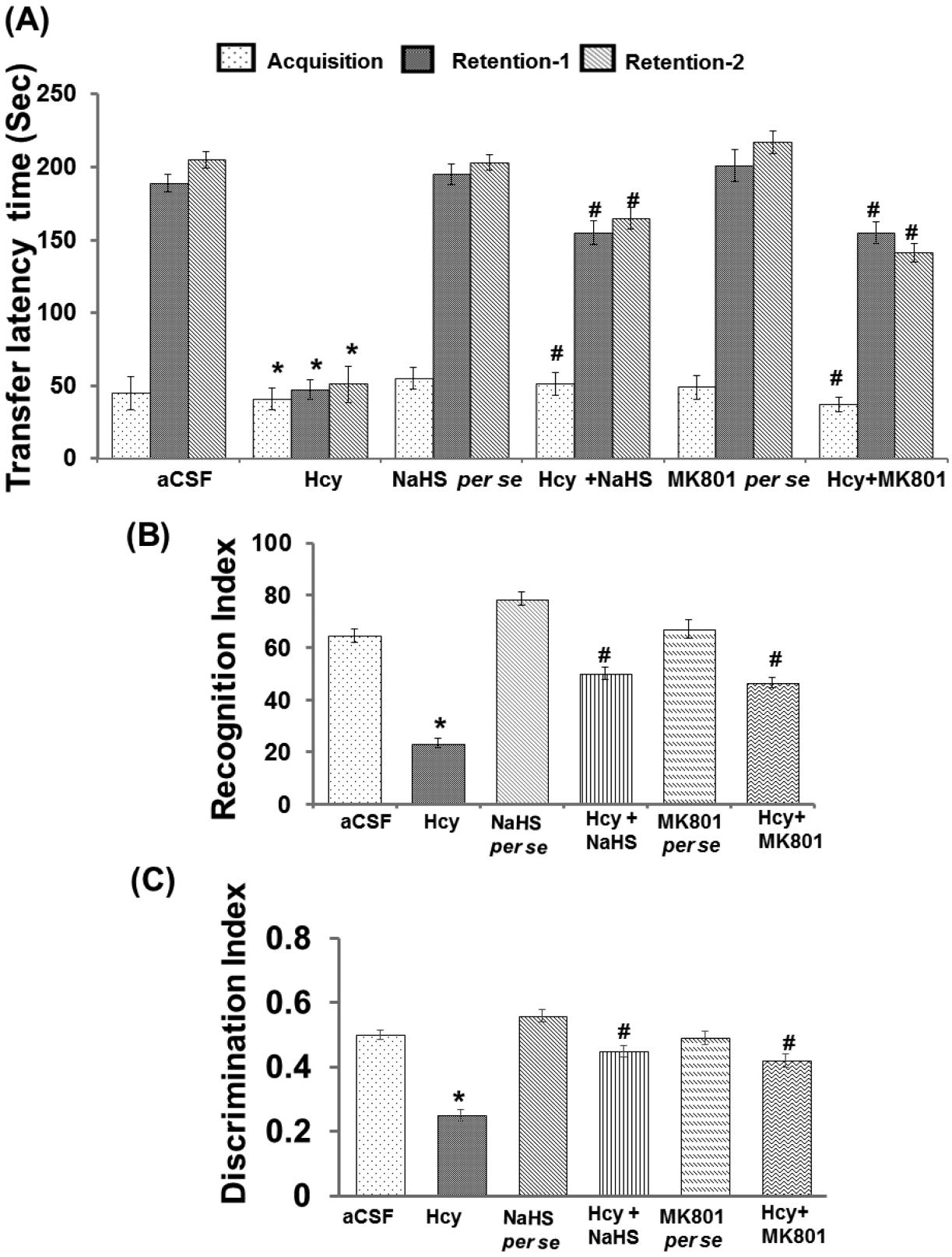

Figure-1.

Memory test using passive avoidance and novel object recognition test in different groups of mice. **A.** Bar graph showing data of passive avoidance test done in different groups of mice, **B.** Bar graph representation of novel object recognition test performed in different groups of mice. **C.** Bar graph represents the Discrimination index performed in different groups of mice. A p value *$p<0.05$ indicates significance of difference between control verses Hcy (IC) treatment. A p value #$p<0.05$ indicates significance of difference between homocysteine (Hcy) verses NaHS and MK801 treatment.

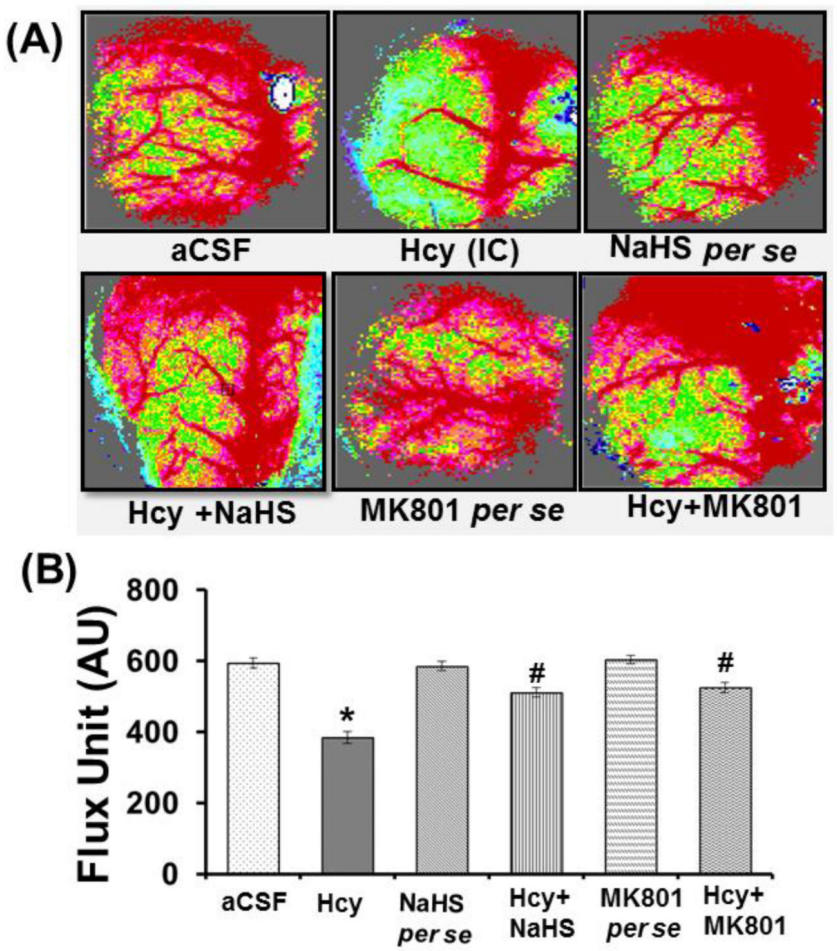

Figure-2.

A. Representative Images showing microvascular density in brain using laser Doppler flow in different groups of mice. **B.** Line diagram representing flux units of microvascular density captured in the 6 different areas in the cranial window prepared in different groups of mice. A p value *p<0.05 indicates significance of difference between control verses Hcy (IC) treatment. A p value #p<0.05 indicates significance of difference between homocysteine (Hcy) verses NaHS and MK801 treatment.

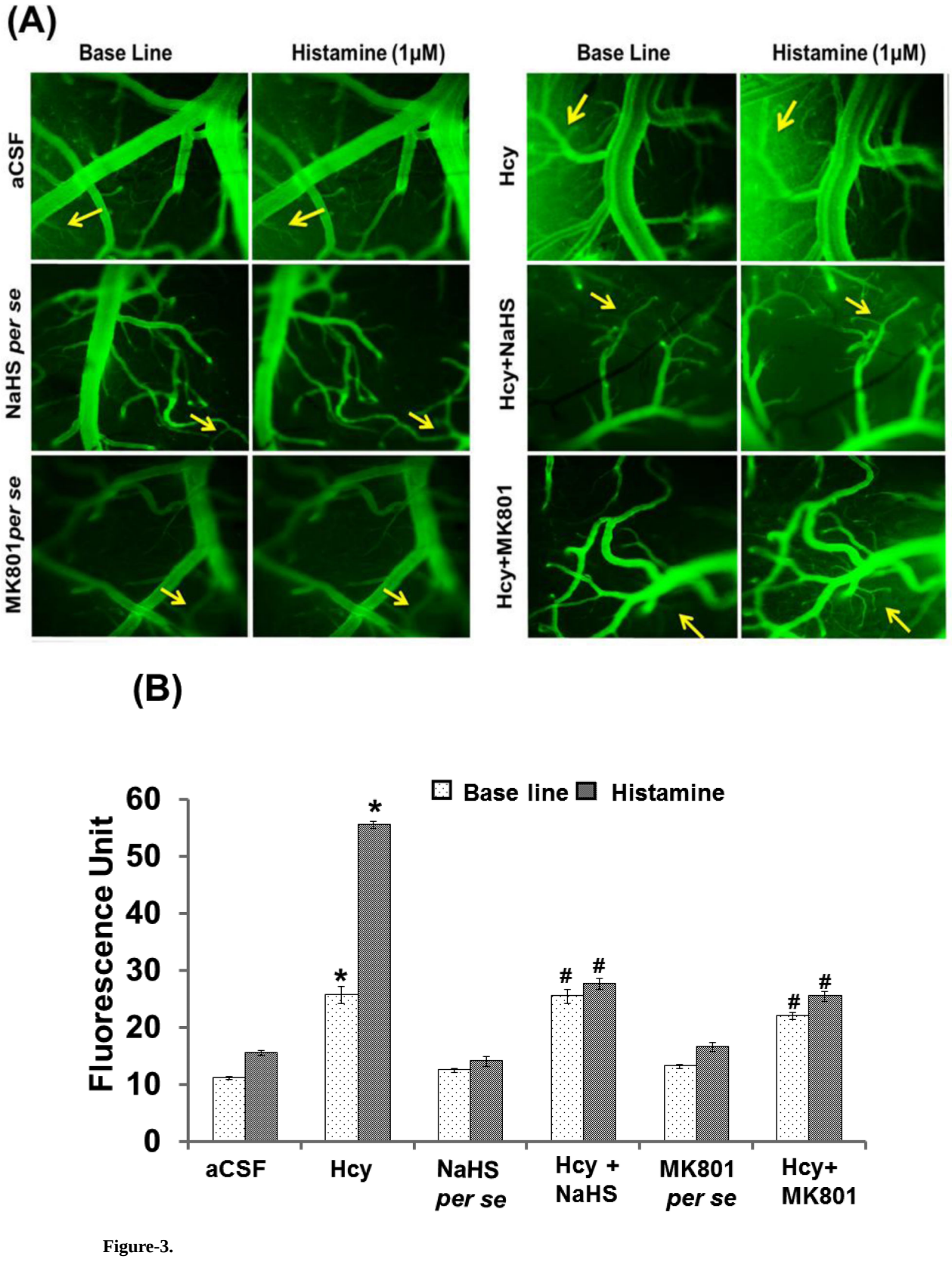

Figure-3.

A. Images showing microvascular permeability in cerebral vessels by infusion of FITC-BSA. The first vertical lane captured base line images and the adjacent lanes are representing vascular permeability by the infusion of BSA-FITC with histamine. **B.** Line diagram showing fluorescent units derived for base line FITC-BSA (green line) and histamine (red line) infused through carotid artery. A p value *$p<0.05$ indicates significance of difference between control verses Hcy (IC) treatment. A p value #$p<0.05$ indicates significance of difference between homocysteine (Hcy) verses NaHS and MK801 treatment.

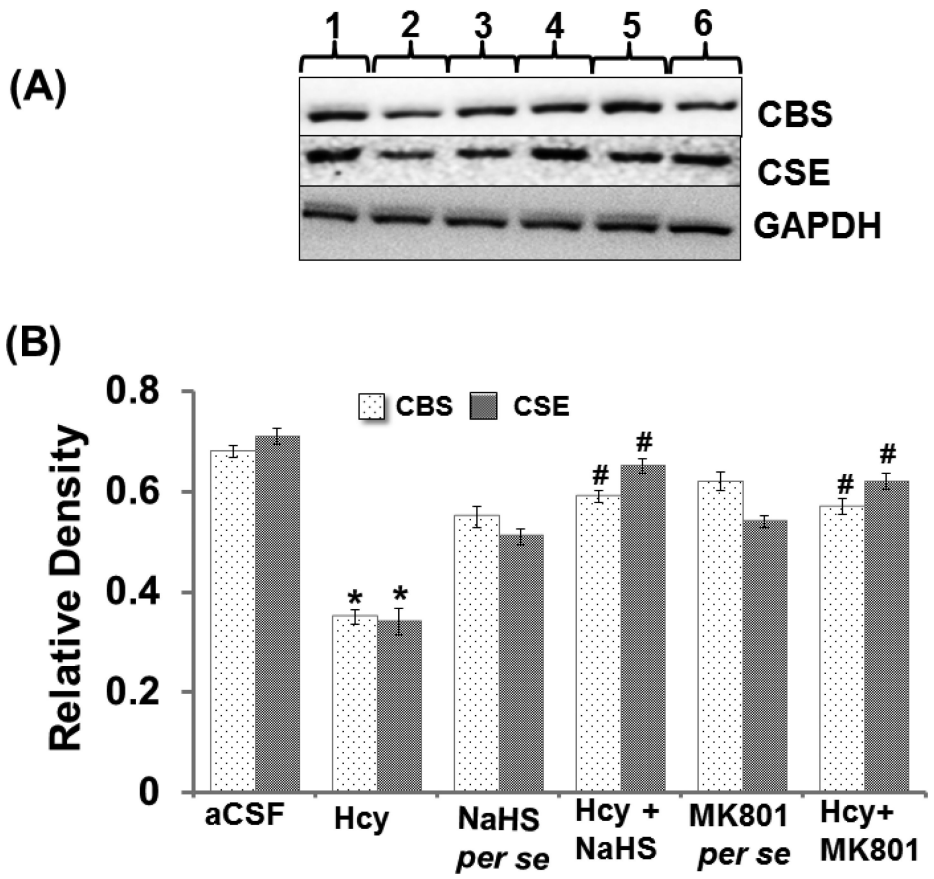

Figure-4.

A. Representative Western blot images for CBS, CSE and GAPDH in different groups of mice. Here, **1.** aCSF, **2.** Hcy, **3.** NaHS *per se*, **4.** Hcy+NaHS, **5.** MK801 *per se*, **6.** Hcy +MK801. **B.** Bar graph images showing data for quantitative estimation of CBS and CSE in different groups of mice after normalization with housekeeping protein GAPDH. A p value *p<0.05 indicates significance of difference between control verses Hcy (IC) treatment. A p value #p<0.05 indicates significance of difference between homocysteine (Hcy) verses NaHS and MK801 treatment.

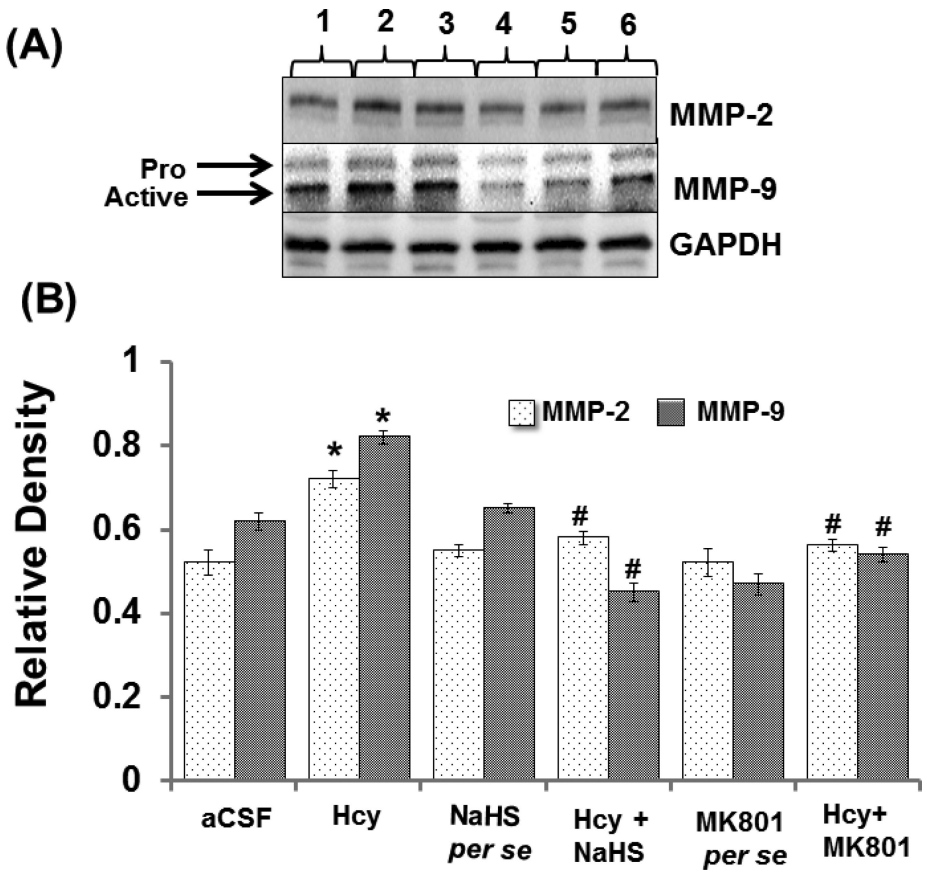

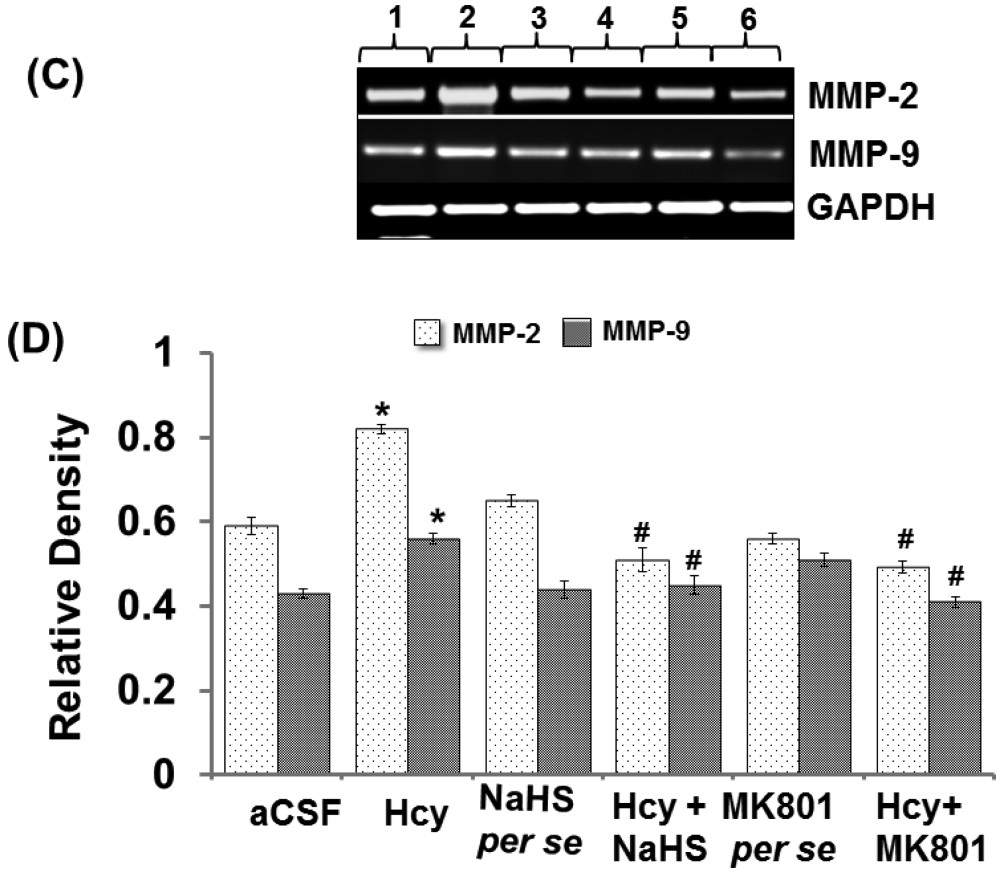

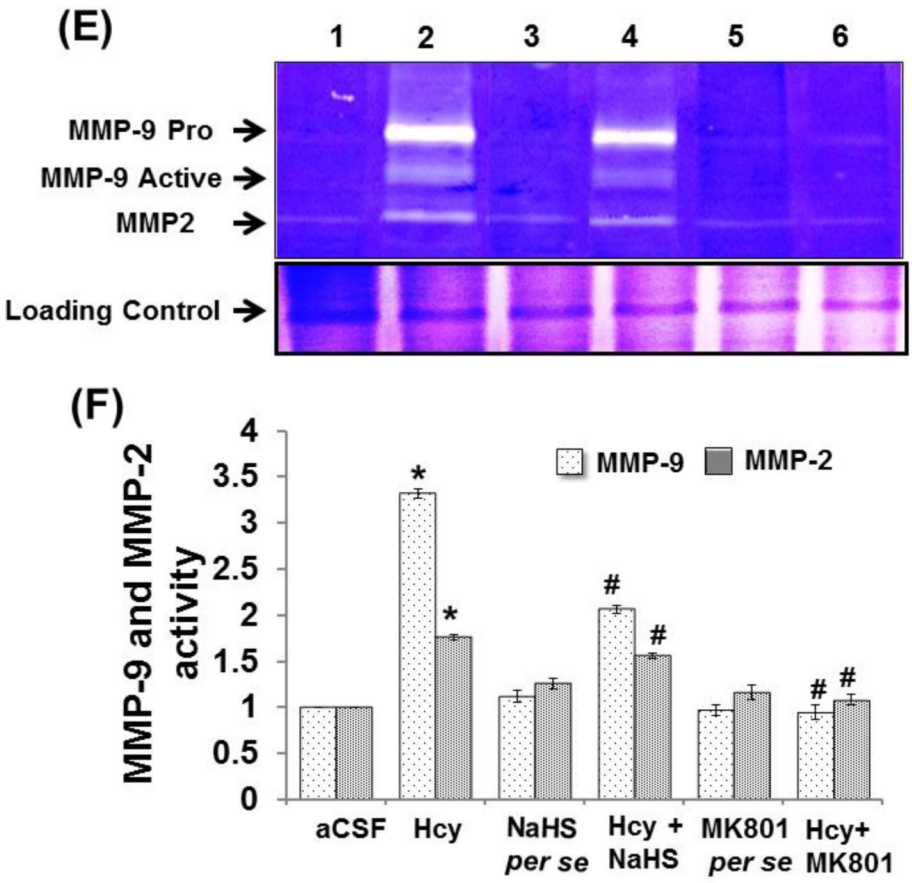

Figure-5.

A. Representative Western blot images showing the levels of matrix metalloproteae-2 and, -9 (MMP-2 and MMP-9) with GAPDH in different groups of mice. Here, **1.** aCSF, **2.** Hcy, **3.** NaHS *per se*, **4.** Hcy+NaHS, **5.** MK801 *per se*, **6.** Hcy+MK801. **B.** Bar graph images showing data for quantitative estimation of MMP-2 and MMP-9 in different groups of mice. The levels of the two gelatinases were normalized with GAPDH levels of respective groups of mice. A p value *p<0.05 indicates significance of difference between control verses Hcy (IC) treatment. A p value #p<0.05 indicates significance of difference between homocysteine (Hcy) verses NaHS and MK801 treatment.

Figure-5: C. Representative RT-PCR images results showing the levels of MMP-2 and MMP-9 mRNA with GAPDH mRNA in different groups of mice. Here, **1.** aCSF, **2.** Hcy, **3.** NaHS *per se*, **4.** Hcy+NaHS, **5.** MK801 *per se*, **6.** Hcy+MK801. **D.** Bar graph showing data for quantitative estimations of MMP-2 and MMP-9 mRNA levels in different groups of mice after normalization with housekeeping mRNA GAPDH. *p<0.05 *vs.* control, #p<0.05 *vs.* Hcy. A p value *p<0.05 indicates significance of difference between control verses Hcy (IC) treatment. A p value #p<0.05 indicates significance of difference between homocysteine (Hcy) verses NaHS and MK801 treatment.

Figure-5: E. Representative gelatin zymography images of MMP-9 and MMP-2 gelatinolytic activities in different groups of mice. Here, **1.** aCSF, **2.** Hcy, **3.** NaHS *per se*, **4.** Hcy+NaHS, **5.** MK801 *per se*, **6.** Hcy+MK801. Lower images showing the data for the SDS-PAGE of protein extracts isolated from respective groups of mice. **F.** Bar graph showing the

gelatinolyic activity of MMP-2 and MMP-9 in different groups of mice. A p value *p<0.05 indicates significance of difference between control verses Hcy (IC) treatment. A p value #p<0.05 indicates significance of difference between homocysteine (Hcy) verses NaHS and MK801 treatment.

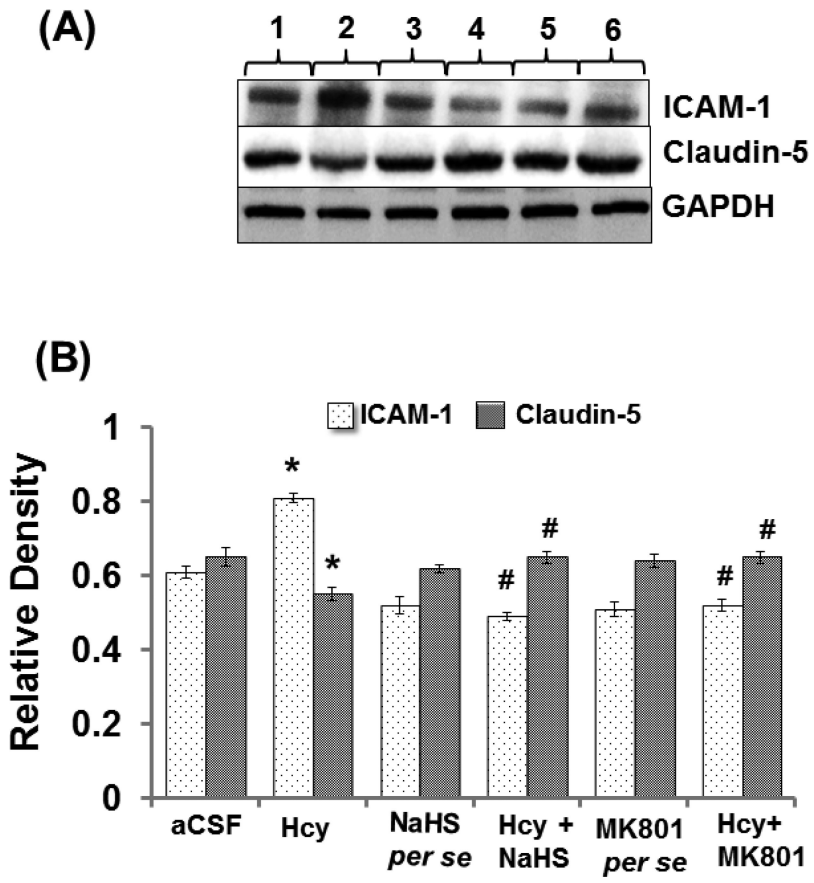

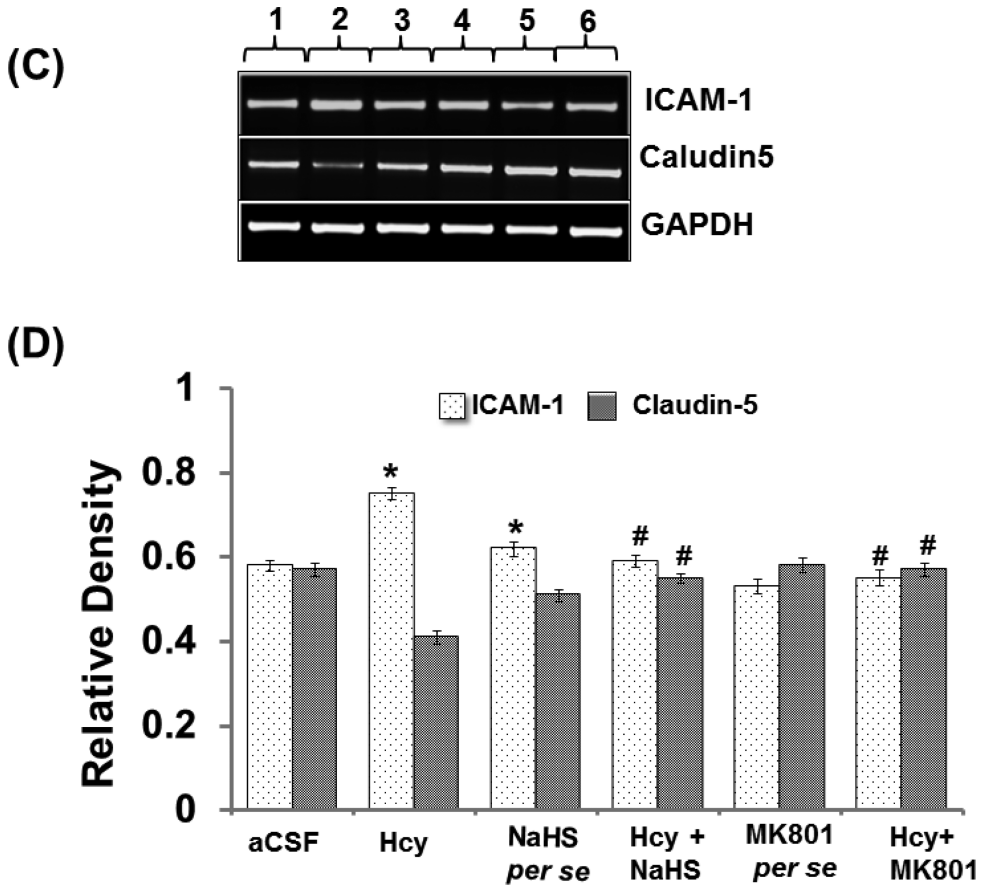

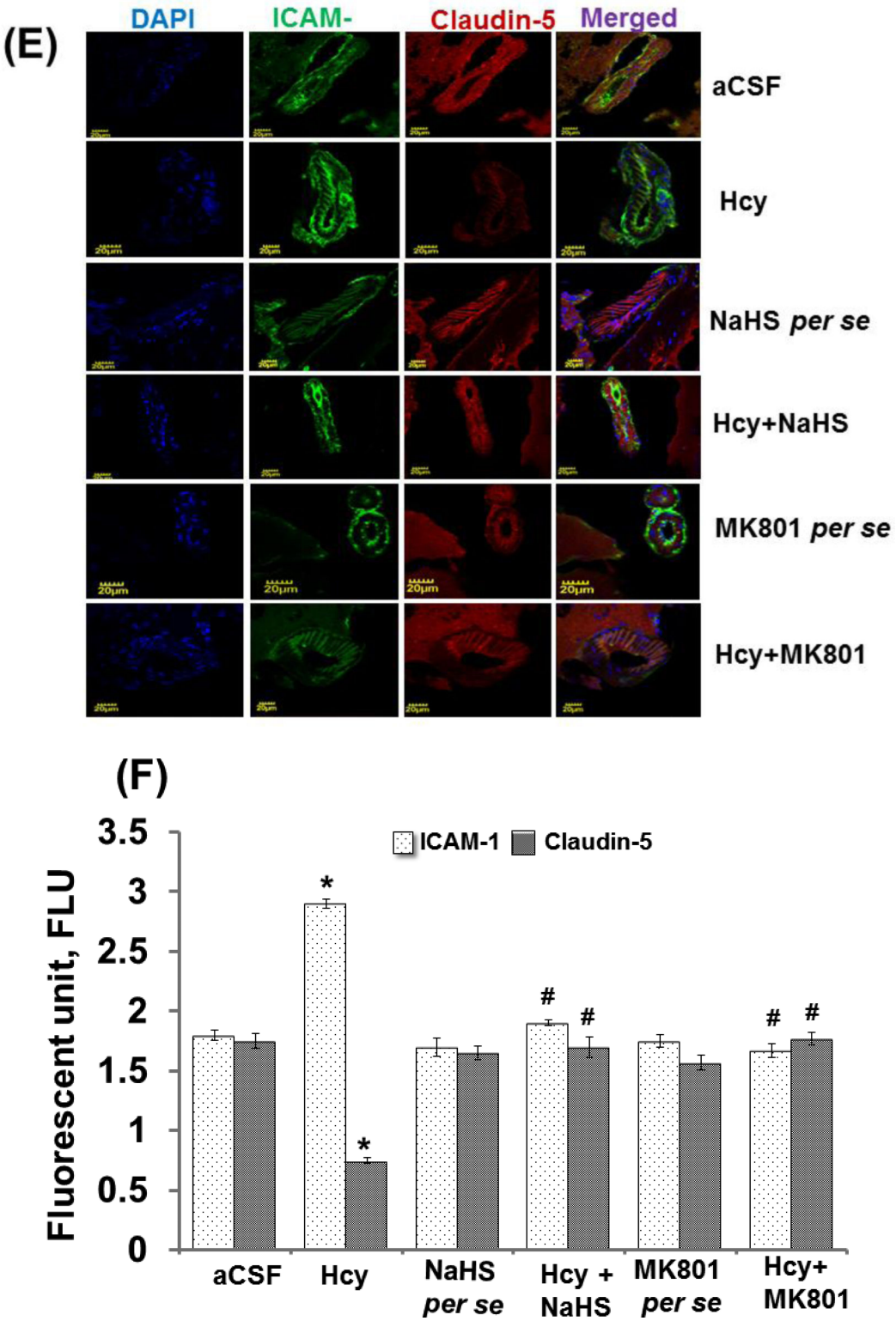

Figure-6.

A. Representative Western blot images of ICAM, claudin-5 and GAPDH in different groups of mice. Here, **1.** aCSF, **2.** Hcy, **3.** NaHS *per se*, **4.** Hcy+NaHS, **5.** MK801 *per se*, **6.** Hcy

+MK801. **B.** Bar graph showing the protein expression levels of ICAM, claudin-5 normalized with GAPDH in different groups of mice. A p value *p<0.05 indicates significance of difference between control verses Hcy (IC) treatment. A p value #p<0.05 indicates significance of difference between homocysteine (Hcy) verses NaHS and MK801 treatment.

Figure-6: C. Representative RT-PCR images of ICAM, claudin-5 and GAPDH mRNA in different groups of mice. Here, **1.** aCSF, **2.** Hcy, **3.** NaHS *per se*, **4.** Hcy+NaHS, **5.** MK801 *per se*, **6.** Hcy+MK801. **D.** Bar graph representing the expression levels of ICAM, claudin-5 normalized with GAPDH mRNA expression levels in different groups of mice. A p value *p<0.05 indicates significance of difference between control verses Hcy (IC) treatment. A p value #p<0.05 indicates significance of difference between homocysteine (Hcy) verses NaHS and MK801 treatment.

Figure-6: E. Confocal images of ICAM and claudin -5 stained cerebral cortical vessels. First lane representing DAPI stained nuclei (blue), second lane representing ICAM (green), third lane showing tight junction claudin-5 (red) and the fourth lane expressing the merged images of the three lanes. **F.** Bar graph representing the quantitative fluorescence expressions of ICAM and cladin-5. A p value *p<0.05 indicates significance of difference between control verses Hcy (IC) treatment. A p value #p<0.05 indicates significance of difference between homocysteine (Hcy) verses NaHS and MK801 treatment.

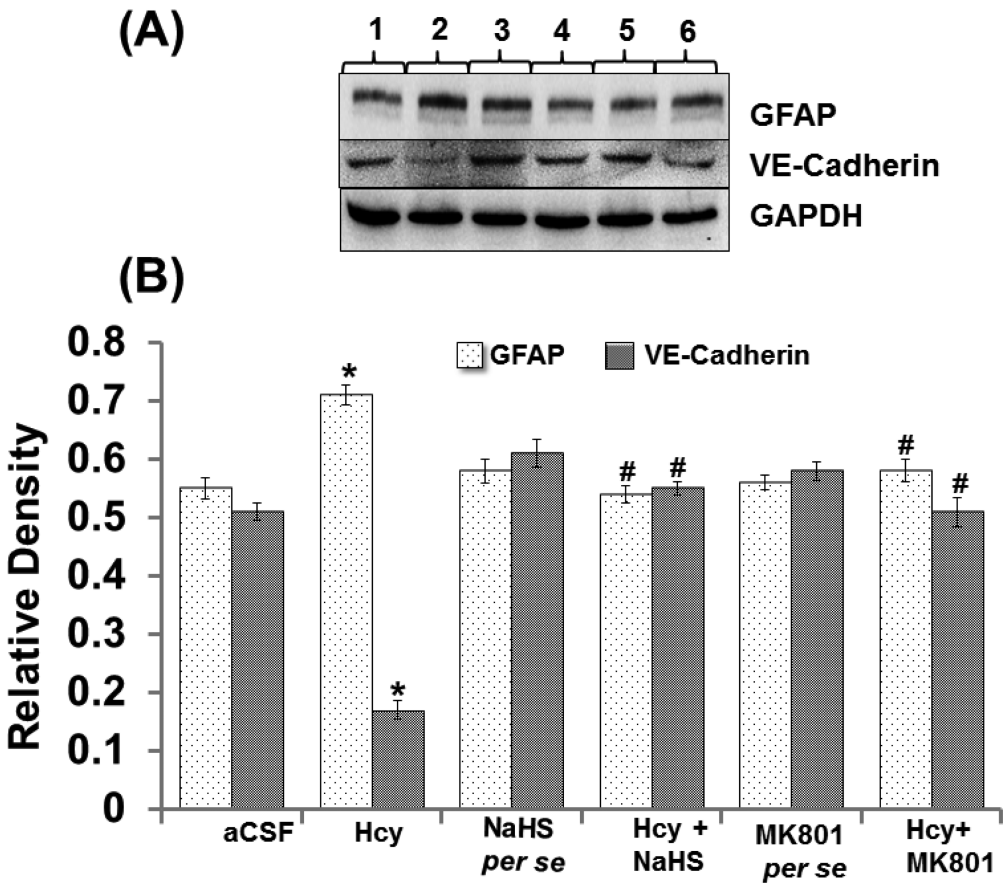

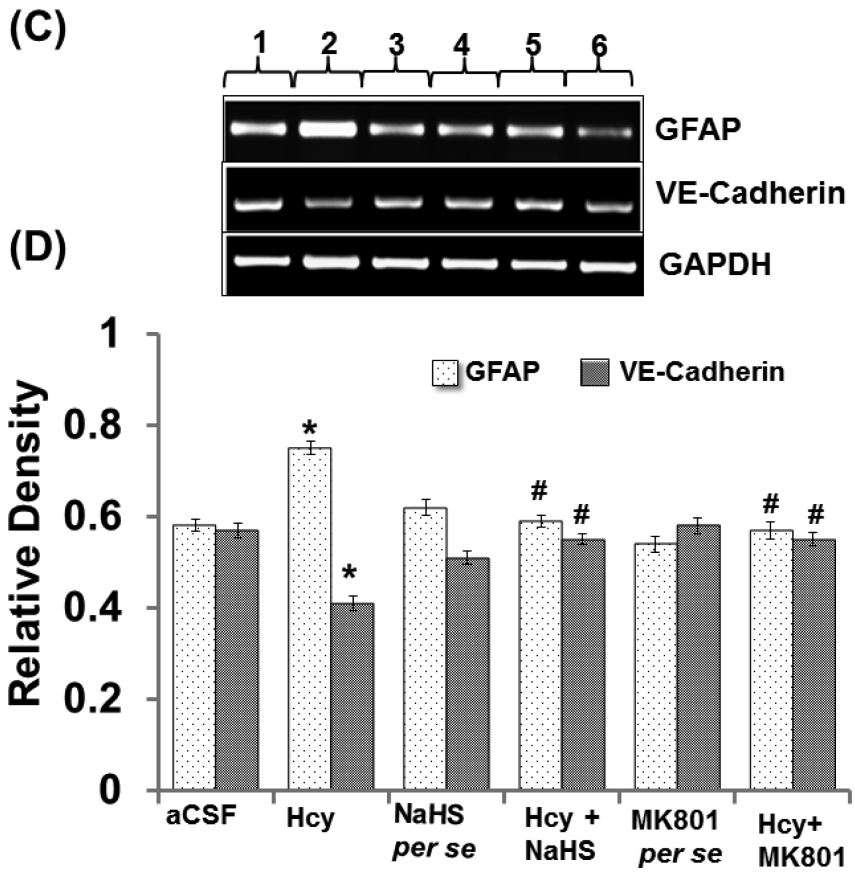

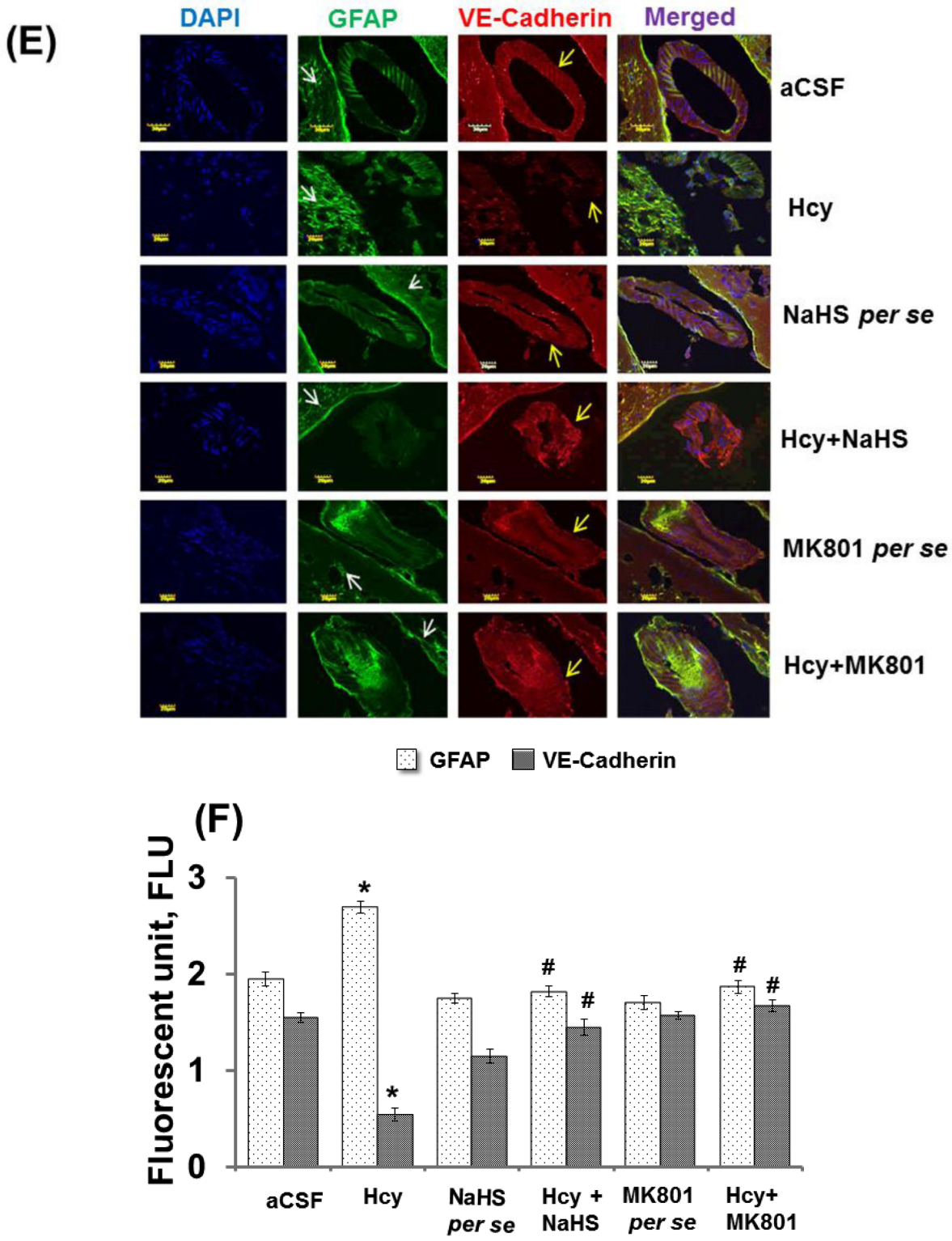

Figure-7.

A. Representative Western blot images of GFAP, VE-cadherin and GAPDH in different groups of mice. Here, **1.** aCSF, **2.** Hcy, **3.** NaHS *per se*, **4.** Hcy+NaHS, **5.** MK801 *per se*, **6.**

Hcy+MK801. **B.** Bar graph showing the protein expression levels of GFAP, VE-cadherin normalized with GAPDH in different groups of mice. Figure **C**. Representative RT-PCR analysis of GFAP, VE-cadherin and GAPDH in different groups of mice. Here, **1.** aCSF, **2.** Hcy, **3.** NaHS *per se*, **4.** Hcy+NaHS, **5.** MK801 *per se*, **6.** Hcy+MK801. **D.** Bar graph representing the mRNA expression levels of GFAP, VE-cadherin normalized with GAPDH in different groups of mice. A p value *p<0.05 indicates significance of difference between control verses Hcy (IC) treatment. A p value #p<0.05 indicates significance of difference between homocysteine (Hcy) verses NaHS and MK801 treatment.

Figure-7 E: Confocal images of GFAP (green) and VE-cadherin (red) stained cerebral cortical vessels. First lane representing DAPI stained nuclei (blue), second lane representing GFAP, third lane showing adherent junction VE-cadherin (red) and the fourth lane expressing the merged images of the three lanes. **F.** Bar graph representing the quantitative fluorescence expressions of GFAP and VE-cadherin. A p value *p<0.05 indicates significance of difference between control verses Hcy (IC) treatment. A p value #p<0.05 indicates significance of difference between homocysteine (Hcy) verses NaHS and MK801 treatment.

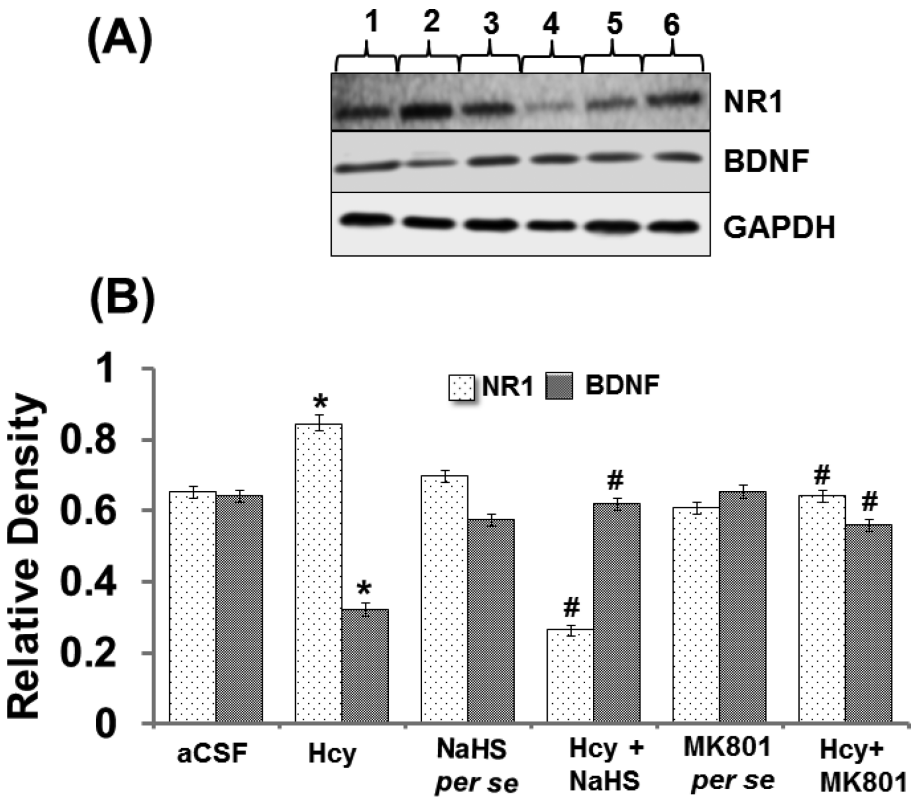

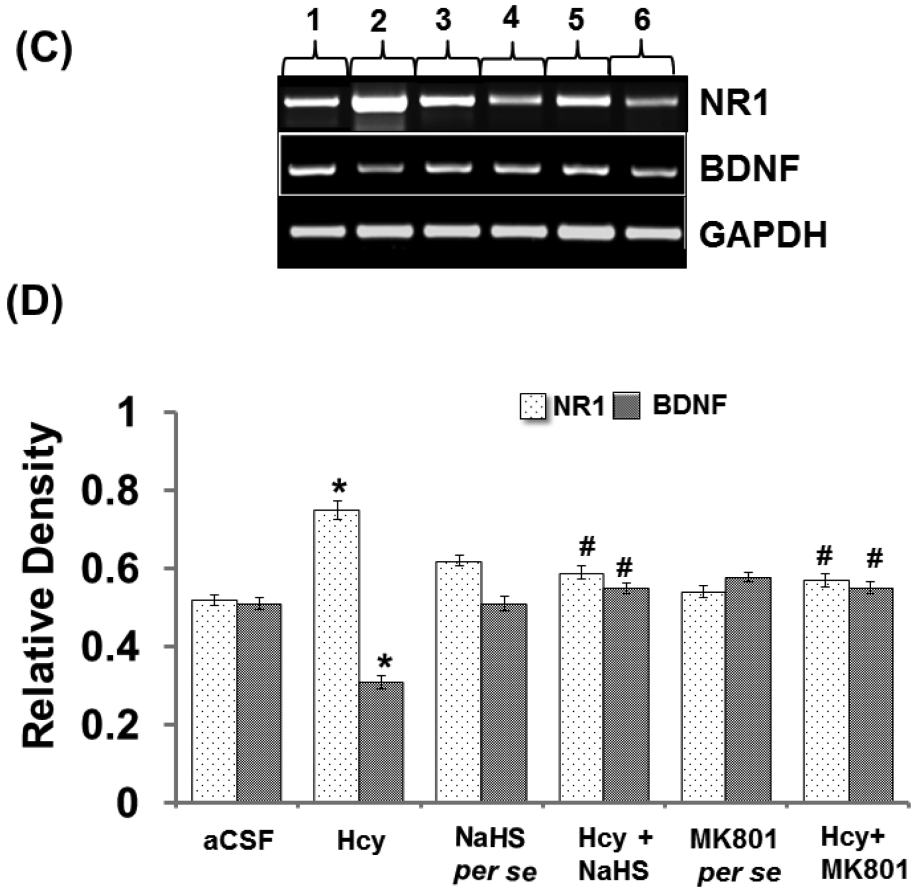

Figure-8.

A. Representative Western blot images of NR-1, BDNF and GAPDH in different groups of mice. Here, **1.** aCSF, **2.** Hcy, **3.** NaHS *per se*, **4.** Hcy+NaHS, **5.** MK801 *per se*, **6.** Hcy +MK801. **B.** Bar graph showing the protein expression levels of NR-1 and BDNF normalized with GAPDH in different groups of mice. Figure **C**. Representative RT-PCR analysis of NR-1, BDNF and GAPDH in different groups of mice. Here, **1.** aCSF, **2.** Hcy, **3.** NaHS *per se*, **4.** Hcy+NaHS, **5.** MK801 *per se*, **6.** Hcy+MK801. **D.** Bar graph representing the mRNA expression levels of NR-1, BDNF normalized with GAPDH in different groups of mice. A p value *p<0.05 indicates significance of difference between control verses Hcy (IC) treatment. A p value #p<0.05 indicates significance of difference between homocysteine (Hcy) verses NaHS and MK801 treatment.

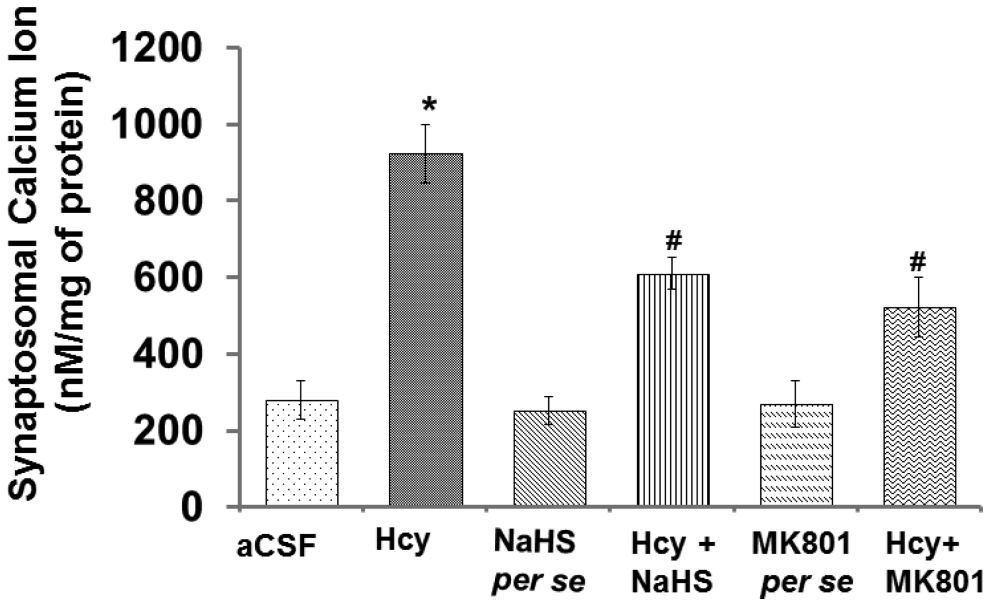

Figure-9.

Bar graph representing synaptosomal calcium levels in different groups of mice. The values for calcium quantitation represent in nM/mg of protein. A p value *p<0.05 indicates significance of difference between control verses Hcy (IC) treatment. A p value #p<0.05 indicates significance of difference between homocysteine (Hcy) verses NaHS and MK801 treatment.

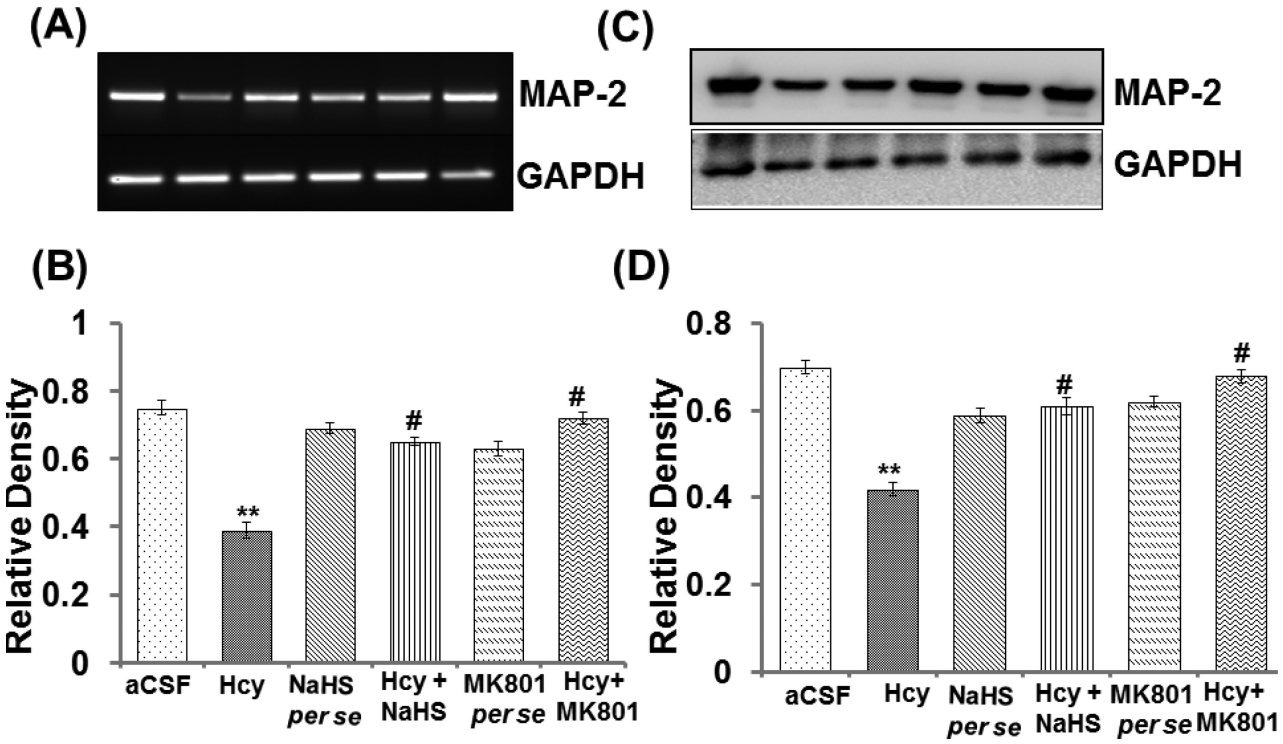

Figure-10.

A. PCR and C. Western blot image showing the expression of MAP-2 and graph B and D represent the level of expression of MAP-2 in different treated group. A p value *p<0.05 indicates significance of difference between control verses Hcy (IC) treatment. A p value #p<0.05 indicates significance of difference between homocysteine (Hcy) verses NaHS and MK801 treatment.

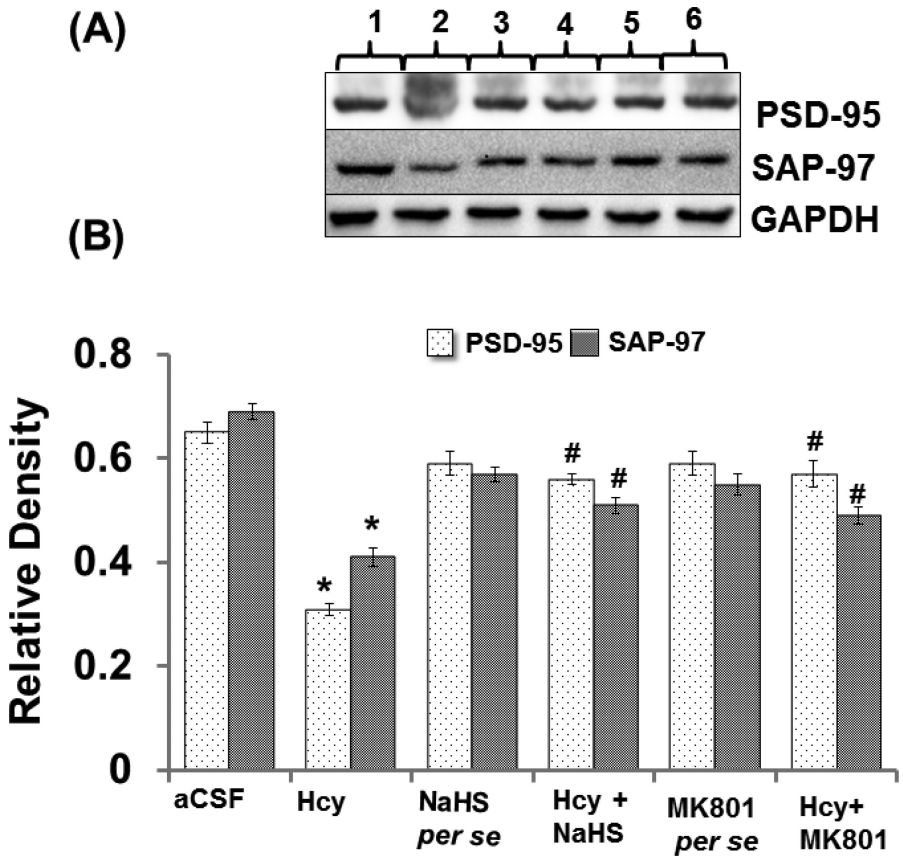

Figure-11.

Representative Western blot images of PSD-95, SAP-97 and GAPDH in different groups of mice. Here, **1.** aCSF, **2.** Hcy, **3.** NaHS *per se*, **4.** Hcy+NaHS, **5.** MK801 *per se*, **6.** Hcy +MK801. **B.** Bar graph showing the protein expression levels of PSD-95, SAP-97 normalized with GAPDH in different groups of mice A p value *p<0.05 indicates significance of difference between control verses Hcy (IC) treatment. A p value #p<0.05 indicates significance of difference between homocysteine (Hcy) verses NaHS and MK801 treatment.

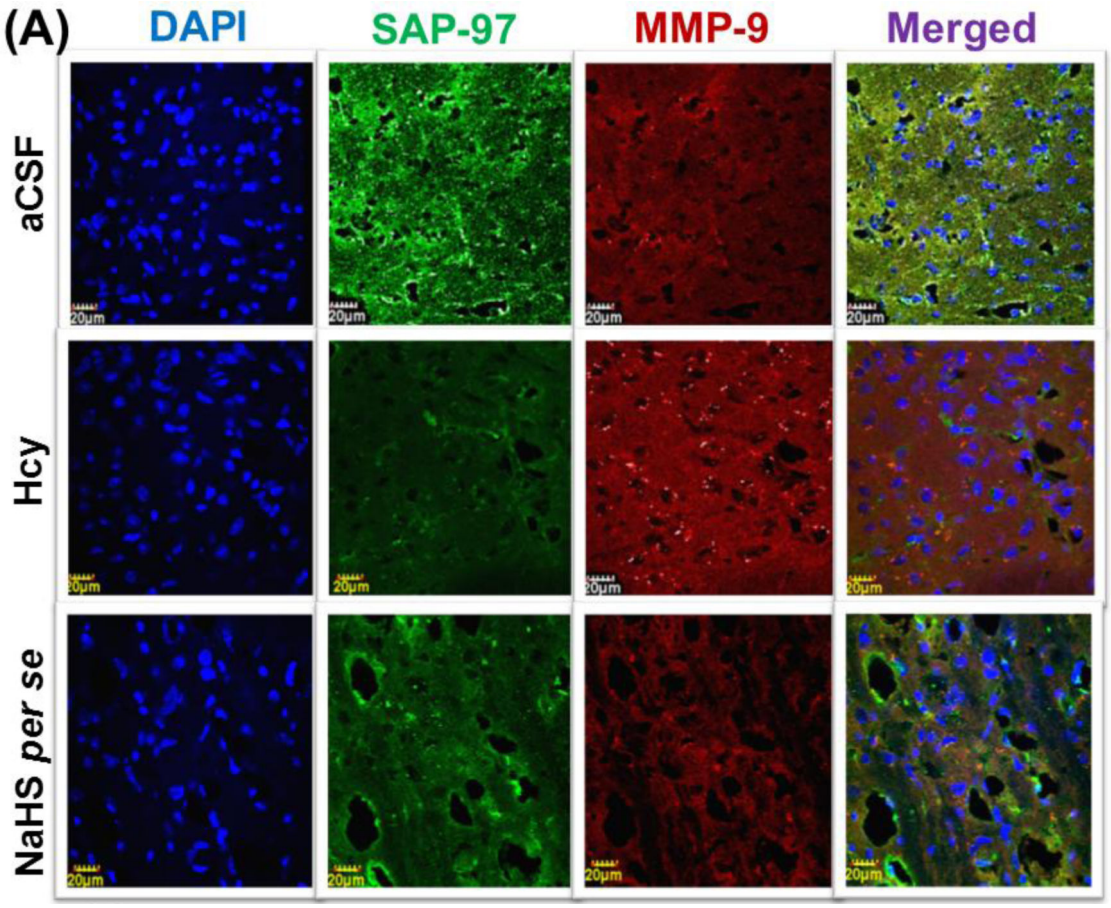

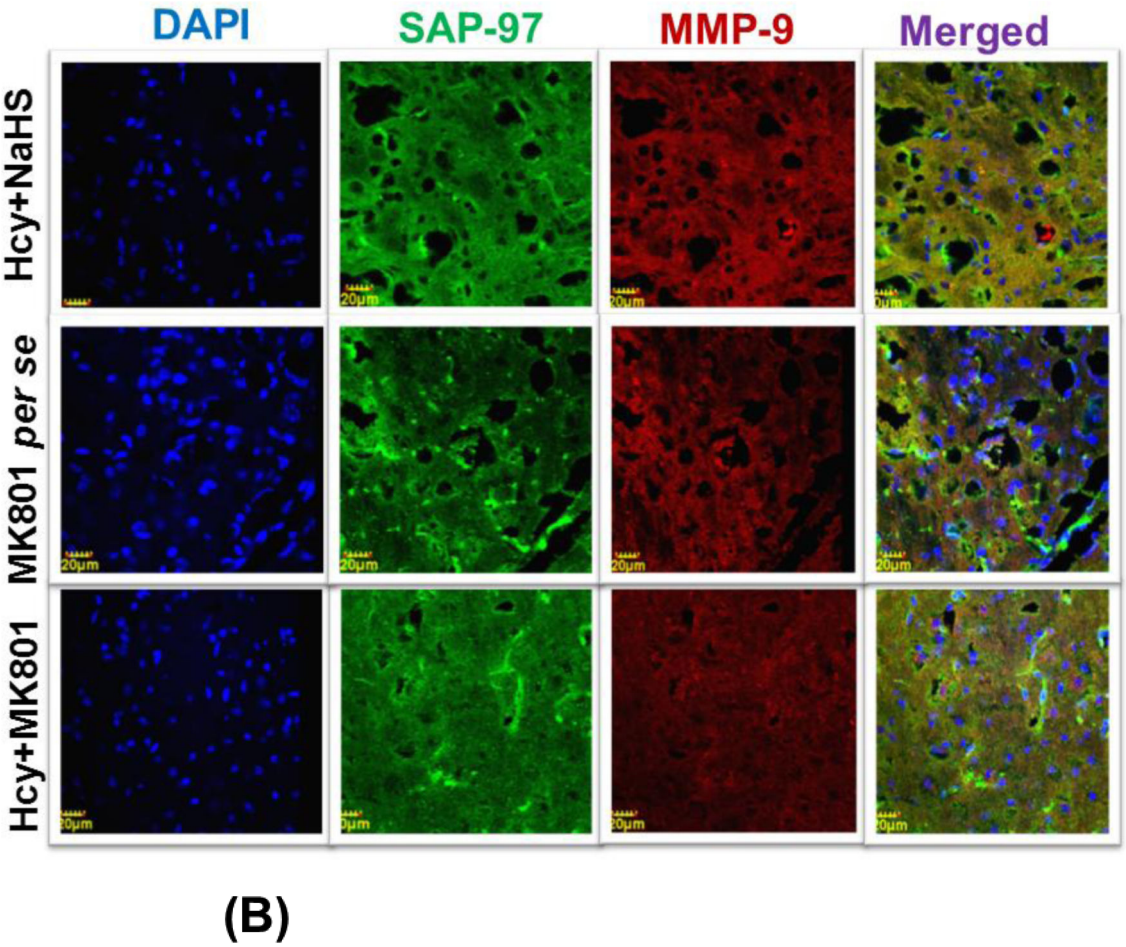

(B)

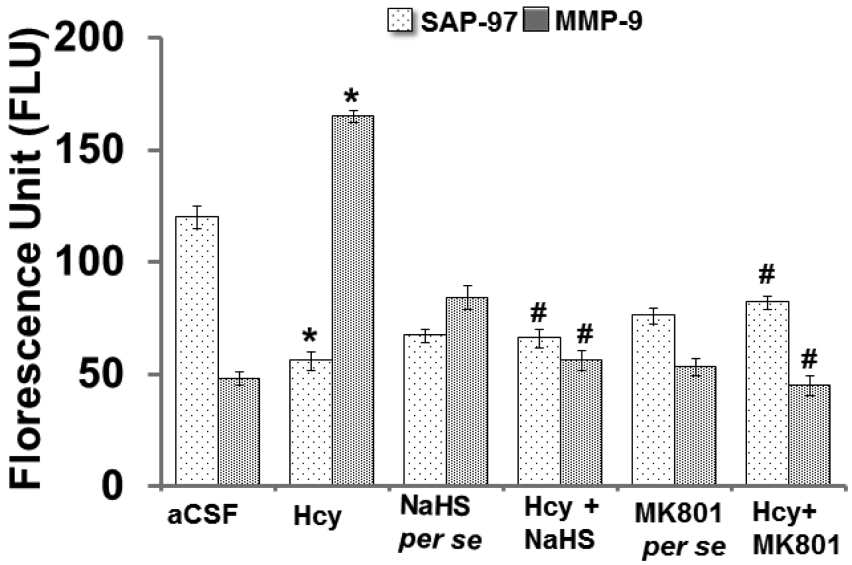

Figure-12.

Confocal images of SAP-97 (green) and MMP-9 (red) stained cerebral cortical region. First lane representing DAPI stained nuclei (blue), second lane representing SAP-97, third lane showing MMP-9 and the fourth lane expressing the merged images of the three lanes. **B.** Bar graph representing the quantitative fluorescence expressions of SAP-97 and MMP-9. A p value *$p<0.05$ indicates significance of difference between control verses Hcy (IC) treatment. A p value #$p<0.05$ indicates significance of difference between homocysteine (Hcy) verses NaHS and MK801 treatment.

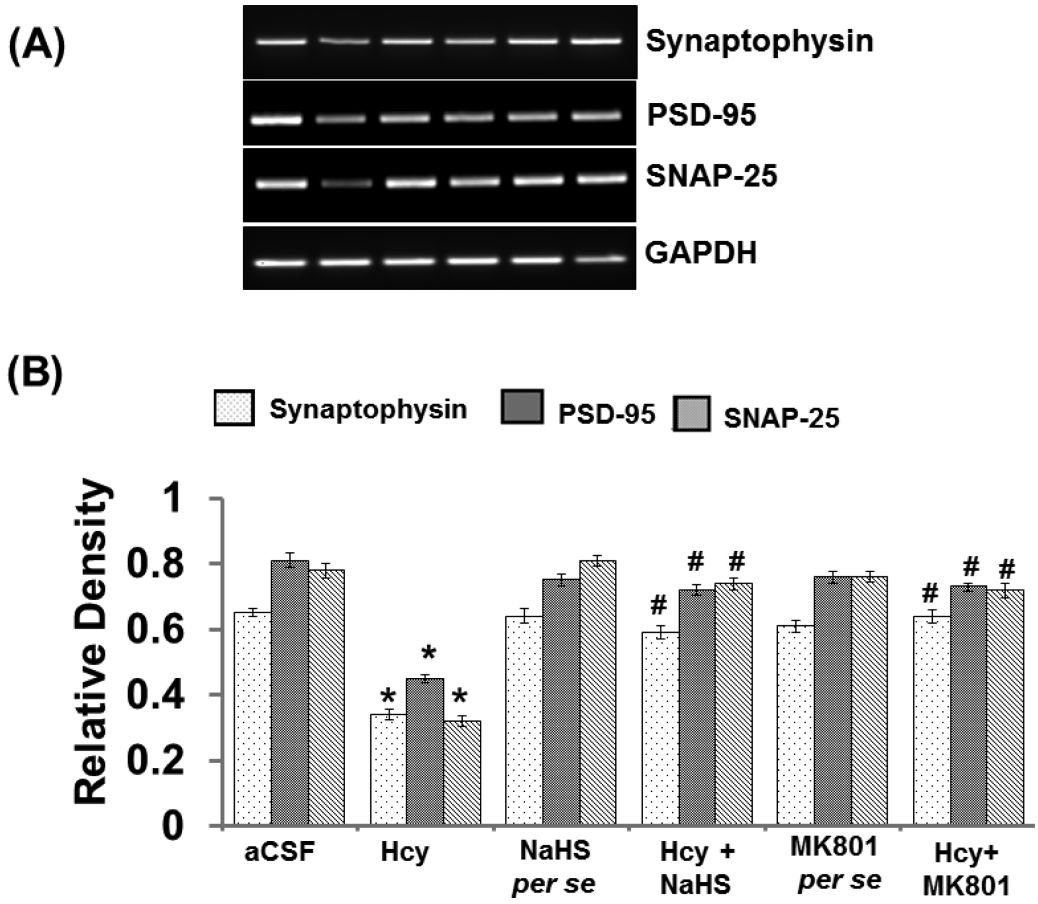

Figure-13.

Representative RT-PCR images of synapse-related proteins synaptophysin, PSD-95, SNAP-25 and GAPDH in different groups of mice. Here, **1.** aCSF, **2.** Hcy, **3.** NaHS *per se*, **4.** Hcy+NaHS, **5.** MK801 *per se*, **6.** Hcy+MK801. **B.** Bar graph showing the mRNA expression levels of synaptophysin, PSD-95, SNAP-25 normalized with GAPDH in different groups of mice. A p value *p<0.05 indicates significance of difference between control verses Hcy (IC) treatment. A p value #p<0.05 indicates significance of difference between homocysteine (Hcy) verses NaHS and MK801 treatment.

Table 1

represents the sequence of primers of the different genes and their product length.

Primers	Forward sequence	Reverse sequence	Base pair
PSD95	5′-CAAGACCGACATCACAGGA-3′	5′-ACGGCAAGGGCGAAT-3′	470
SNAP25	5′-GCAGGGTAACAAACGATGCC-3	5′-CTTCCCAGCATCTTTGTTGC-3′	211
Synaptophysin	5′-TGCAGAACAAGTACCGAGAG-3′	5′-CTGTCTCCTTAAACACGAACC-3′	297
MAP-2	5′-CCACCTGAGATTAAGGATCA-3′	5′-GGCTTACTTTGCTTCTCTGA-3′	482
MMP-2	5′ –GCACTCTGGAGCGAGGATAC-3′	5′-GCCCTCCTAAGCCAGTCTCT-3′	362
MMP-9	5′-AAGGCAAACCCTGTGTGTTC-3′	5′-GTGGTTCAGTT GTGGTGGTG-3′	385
ICAM-1	5′-GTGGCGGGAAAGTTCCTG-3′	5′-CGTCTTGCAGGTCATCTTAGGAG-3′	171
Claudin-5	5′-GGCACTCTTTGTTACCTTGACC-3′	5′-CAGCTCGTACTTCTGTGACACC-3′.	202
GFAP	5′-TCCTGGAACAGCAAAACAAG-3′	5′-CAGCCTCAGGTTGGTTCAT-3′	256
VE-Cadherin	5′-AACTTCCCCTTCTTCACCC-3′	5′-AAAGGCTGCTGGAAAATG-3′	512
NR1	5′-GAATGATGGGCGAGCTACTCA-3′	5′-ACGCTCATTGTTGATGGTCAGT-3′	71
BDNF	5′- GGGTCACAGCGGCAGATAAA -3′	5′- GCCTTTGGATACCGGGACTT -3′.	86
GAPDH	5′-TGAAGGTCGGTGTGAACGGATTTGGC-3′	5′-CATGTAGGCCATGAGGTCCACCAC-3′	983